PACIFIC ISLANDS APPLIED GEOSCIENCE COMMISSION

Oceanographic Survey, Shoreline Mapping and Preliminary Hydrodynamic Modelling Report, Saipan, Commonwealth of the Northern Mariana Islands Data Acquisition undertaken from April to July 2010

SOPAC Data Release Report 26
September 2010

Jens Krüger, Salesh Kumar, Herve Damlamian, and Ashishika Sharma
Ocean & Islands Programme, SOPAC

PACIFIC ISLANDS APPLIED GEOSCIENCE COMMISSION
c/o SOPAC Secretariat
Private Mail Bag
GPO, Suva
FIJI ISLANDS
http://www.sopac.org
Phone: +679 338 1377
Fax: +679 337 0040
www.sopac.org
director@sopac.org

Financial support for this report was provided by the Coastal Zone Management Act of 1972, as amended, administered by the Office of Ocean and Coastal Resource Management, National Oceanic and Atmospheric Administration.

Table of Contents

List of Figures 2
Acknowledgements 8
1 Introduction 10
2 Methods 11
2.1 Current Meter Deployments 11
2.2 Wave Gauge Deployments 14
2.3 GNSS Reef and Shoreline Survey 16
2.4 GPS Photo Shoreline Mapping 19
2.5 Sediment Sampling 20
2.6 Oceanography and Meteorology 23
2.7 Wave-Current Hydrodynamic Model 24
3 Results 28
3.1 ADP Channel 28
3.2 ADP Lagoon 30
3.3 ADV Managaha Island 32
3.4 AWAC Outfall 34
3.5 TWR Reef Slope North 36
3.6 TWR Reef Flat North 37
3.7 TWR Reef Slope South 38
3.8 TWR Reef Flat South 39
3.9 Meteorological Data, Saipan Airport Station 40
3.10 ECMWF ERA-Interim Metocean data 41
3.11 GNSS Survey Data 46
3.12 Geocoded Photos 48
3.13 Sediment Samples 54
3.14 Wave-Current Hydrodynamic Model 58
4 References 63

List of Figures

Figure 1. Map of Saipan and the location of field sites. The backdrop is an unrectified 2005 Quickbird satellite image provided by CRMO. 10
Figure 2. Mooring locations within Saipan Lagoon. Mooring stations are indicated by triangles. Background image is an unrectified 2005 Quickbird image provided by CRMO. 11
Figure 3. Nortek 600kHz AWAC-AST in preparation for deployment. The blue canister in the foreground is the external battery compartment. The black cylinder to the right is the acoustic release. The transducer head itself is shown sitting at the centre top of the aluminium tripod. 12
Figure 4. The tide and wave recorder RBR-TWR-2050P (26.5 cm x 3.8 cm overall dimensions) was contained within the protective PVC housing, attached to an aluminium frame, and weighed down with scrap metal, before being placed on the seabed. 15
Figure 5. GNSS survey points. Base stations were set up at the CRMO office building and the University of Hawaii tide gauge survey mark UH2C, which provided vertical control for the survey. Backdrop is an unrectified 2005 Quickbird image supplied by CRMO. 17
Figure 6. Base station on the southwest corner of the flat-topped building of the CRMO office. The unit was levelled on top of an existing timber bar attached to the roof with a nail at its centre (see inset). 18
Figure 7. The two rovers mounted on 2 m survey poles during the shoreline survey at Memorial Park. One receiver can be seen at the vegetated berm to the left, and the

other being held by the surveyor at the toe of the beach..... 18
Figure 8. Tripod and Trimble R8 receiver set up over the tide gauge bench mark at Tanapag Harbour. Observing the tide gauge bench mark provided control for the survey and ensured that post-processed heights were relative to NMVD03. The tide gauge can be seen immediately behind and above the tripod. See Figure 11 for location..... 19
Figure 9. A photo was taken of the handheld GPS displaying the time of day in local standard time at the start of each survey. This enabled geocoding of any subsequent photos by way of matching the GPS location and time with the time stamp embedded in the EXIF information of the JPEG photo file..... 20
Figure 10. Beach sediment sample locations. See table below for more information. Background image is an unrectified Quickbird 2005 image supplied by CRMO. 21
Figure 11. Location of the Saipan Tide gauge (marked by circle) within the grounds of the Port of Saipan where the east parking lot meets with the east face of Delta Dock. .. 23
Figure 12: ECMWF ERA-Interim model data points near Saipan. A 20-year time series of met-ocean data was extracted for grid point 99,50 northeast of Saipan at 147.0°E 16.5°S (position marked by the upper right hand corner balloon)..... 24
Figure 13. Composite bathymetry for Saipan Island, shallow to deep waters (0 to 600 m) are shown as red to blue. This 5 m grid obtained from PIBHMC formed the basis of the bathymetry data for the hydrodynamic model..... 25
Figure 14. An approximately 400 m long representative cross-section perpendicular to the barrier reef north of Managaha Island from the merged dataset obtained from PIBHMC. Note that the plot shows erroneous depths of approximately 3 m below datum along a 50 m section over the shallowest part of the reef. This reef crest area was replaced with depth values of -0.392 m (MLLW) below mean sea level in the model domain..... 25
Figure 15. Mesh grid of the wave model domain. Shallow to deep waters (0 to below 2800 m) are shown as red to purple..... 26
Figure 16. Mesh grid of the hydrodynamic model domain. See Figure 17 for details of the Harbour area. Shallow to deep waters (0 to below 1120 m) are shown as red to purple..... 27
Figure 17. Detail of the hydrodynamic model domain over the northern Saipan Lagoon area. The navigational channel is resolved using a quadrangular mesh and can be seen to the middle left of the image. Mesh size was smallest over the barrier reef depicted by the band along the top of the image, where the maximum length of a mesh segment was constrained to 35 m. Shallow to deep waters (0 to below 140 m) are shown as the colour band from red to purple. 28
Figure 18. Time series plot of depth-averaged current speed and direction measured by the ADP in the channel. Direction is given from true north in oceanographic convention (going toward)..... 29
Figure 19. Time series of temperature as recorded by the ADP in the channel..... 29
Figure 20. Current rose for depth-averaged velocities measured by the ADP in the channel. Directions are shown from true north in oceanographic convention (going toward). Current speeds are given in cm/s..... 30
Figure 21. Scatter density plot of depth averaged current speed and direction measured by the ADP in the channel. Blue to red indicates a range from low to high occurrence of a particular bivariate combination. Direction is given from true north in oceanographic convention (going toward). 30
Figure 22. Time series plot of depth averaged current speed and direction measured by the ADP in the lagoon. Direction is given from true north in oceanographic convention (going toward)..... 31
Figure 23. Time series of temperature as recorded by the ADP in the lagoon. 31
Figure 24. Scatter density plot of depth-averaged current speed and direction measured by the ADP in the lagoon. Blue to red indicates a range from low to high occurrence of a particular bivariate combination. Direction is given from true north in

oceanographic convention (going toward). 32
Figure 25. Current rose for depth averaged velocities (cm/s) measured by the ADP in the lagoon. Directions are shown from true north in oceanographic convention (going toward). 32
Figure 26. Time series plot of water depth, current speed, current direction, and temperature measured by the ADV at Managaha Island. Direction is given from true north in oceanographic convention (going toward). 33
Figure 27. Time series plot of significant wave height (Hs), peak wave period (Tp), wave direction, and directional spread measured by the ADV at Managaha Island. Direction is given from true north in oceanographic convention (going toward). 34
Figure 28. Time series plot of depth-averaged current speed and direction measured by the AWAC near the outfall (see Figure 2 for location). Direction is given from true north in oceanographic convention (going toward). 35
Figure 29. Scatter density plot of depth-averaged current speed and direction measured by the AWAC near the outfall. Blue to red indicates a range from low to high occurrence of a particular bivariate combination. Direction is given from true north in oceanographic convention (going to). 35
Figure 30. Current rose for depth-averaged velocities (cm/s) measured by the AWAC near the outfall. Directions are shown from true north in oceanographic convention (going toward). 36
Figure 31. Time series plot of depth (m), significant wave height (Hs), significant wave period (Ts) and temperature (°C) as measured by the TWR on the northern reef slope. 37
Figure 32. Scatter density plot of significant wave period and wave height for the TWR on the northern reef slope. Blue to red indicates a range from low to high occurrence of a particular bivariate combination. 37
Figure 33. Time series plot of depth (m), significant wave height (Hs), significant wave period (Ts) and temperature (°C) as measured by the TWR on the northern reef flat. 38
Figure 34. Scatter density plot of significant wave period and wave height for the TWR on the northern reef flat. Blue to red indicates a range from low to high occurrence of a particular bivariate combination. 38
Figure 35. Time series plot of depth (m), significant wave height (Hs), significant wave period (Ts) and temperature (°C) as measured by the TWR on the southern reef slope. 39
Figure 36. Scatter density plot of significant wave period and wave height for the TWR on the southern reef slope. Blue to red indicates a range from low to high occurrence of a particular bivariate combination. 39
Figure 37. Time series plot of depth (m), significant wave height (Hs), significant wave period (Ts) and temperature (°C) as measured by the TWR on the southern reef flat. 40
Figure 38. Scatter density plot of significant wave period and wave height for the TWR on the southern reef flat. Blue to red indicates a range from low to high occurrence of a particular bivariate combination. 40
Figure 39. Meteorological parameters collected at the Saipan airport showing time series of air pressure, air temperature, wind speed, and wind direction given in meteorological convention (coming from). 41
Figure 40. Wind rose for the wind speed and direction shown in Figure 39 above. Direction is given in meteorological convention (coming from). Speed is in m/s. 41
Figure 41. ERA-interim Metocean data time series for the period January 1989 to June 2010. Panels from top to bottom are significant wave height (Hs), mean wave period (Tm), mean wave direction (Dm), wind speed (Ws), and wind direction (Wd). Directions are given in oceanographic convention (going toward). 42
Figure 42. Summary plots of ERA-interim wave data. Panels are from left to right and top

to bottom: Panel A shows monthly means and vertical bars of one standard deviation of significant wave height (Hs), mean wave period (Tm), and mean wave direction (Dm); Panel B shows significant wave height in metres and direction as a rose diagram for the entire 20 year dataset; Panel JFM shows a wave rose for the months January, February, and March; Panel AMJ shows the wave rose for April, May and June; Panel JAS shows the wave rose for July, August, and September; and Panel OND shows the wave rose for October, November, and December (OND). Directions are in oceanographic convention (going toward), heights in meters and periods in seconds. 43
Figure 43. Summary plots of ERA-interim wind data. Panels are from left to right and top to bottom: Panel A shows monthly means and vertical bars of one standard deviation of wind speed and direction; Panel B shows a wind rose for the entire 20 year dataset; Panel JFM shows a wind rose for the months January, February, and March; Panel AMJ shows the wind rose for April, May and June; Panel JAS shows the wind rose for July, August, and September; and Panel OND shows the wind rose for October, November, and December (OND). Directions are in oceanographic convention (going toward) and speeds are in m/s. 44
Figure 44: Scatter density plot of mean wave period (Tm), versus significant wave height (Hs) for the ERA-interim dataset. Direction is given from true north in oceanographic convention (going toward). Blue to red indicates a range from low to high occurrence of a particular bivariate combination. 45
Figure 45: Scatter density plot of mean wave period (Tm) versus mean wave direction (Dm) for the ERA-interim dataset. Direction is given from true north in oceanographic convention (going toward). Blue to red indicates a range from low to high occurrence of a particular bivariate combination. 45
Figure 46: Scatter density plot of mean wave direction (Dm) versus significant wave height (Hs) for the ERA-interim dataset. Direction is given from true north in oceanographic convention (going toward). Blue to red indicates a range from low to high occurrence of a particular bivariate combination. 45
Figure 47. Time series of the ERA-interim metocean data for the period 1/5 to Panels from top to bottom show significant wave height (Hs), mean wave period (Tm), mean wave direction (Dm), wind speed (Ws), and wind direction (Wd). 46
Figure 48. Selected spot heights as surveyed on the barrier reef crest in the northern lagoon. Heights are given relative to NMVD 03. Backdrop is an unrectified 2005 Quickbird image supplied by CRMO. 46
Figure 49. Upper beach (pink line) and the toe of beach (yellow line) for Managaha Island. Backdrop is an unrectified 2005 Quickbird image supplied by CRMO. 47
Figure 50. Upper beach (pink line) and the toe of beach (yellow line) for Puntan Muchot (Memorial Park). Backdrop is an unrectified 2005 Quickbird image supplied by CRMO. 47
Figure 51. Upper beach (pink line) and the toe of beach (yellow line) for Sugar Dock. Backdrop is an unrectified 2005 Quickbird image supplied by CRMO. 48
Figure 52. Upper beach (pink line) and the toe of beach (yellow line) for San Antonio. Backdrop is an unrectified 2005 Quickbird image supplied by CRMO. 48
Figure 53. GPS track and geocoded picture thumbnails at Managaha Island displayed from the KMZ file in Google Earth. Clicking on individual or groups of photos causes Google Earth to display larger size pop outs (e.g. the two pictures in the lower right hand corner). Full resolution photos can also be displayed. Geocoded photos were generated with GPicSync (see Methods section for details). 49
Figure 54. Location of geocoded photos by filename at Managaha Island. Geographic coordinates and photos are provided on the Data CD. Backdrop is an unrectified 2003 IKONOS satellite image provided by CRMO. 50
Figure 55. Location of geocoded photos by filename at Puntan Muchot north (Memorial Park). Geographic coordinates and photos are provided on the Data CD. Backdrop is an unrectified 2003 IKONOS satellite image provided by CRMO. 51

Figure 56. Location of geocoded photos by filename at Puntan Muchot south. Geographic coordinates and photos are provided on the Data CD. Backdrop is an unrectified 2003 IKONOS satellite image provided by CRMO. 51
Figure 57. Location of geocoded photos by filename at Sugar Dock north. Geographic coordinates and photos are provided on the Data CD. Backdrop is an unrectified 2003 IKONOS satellite image provided by CRMO. 52
Figure 58. Location of geocoded photos by filename south of Sugar Dock. Geographic coordinates and photos are provided on the Data CD. Backdrop is an unrectified 2003 IKONOS satellite image provided by CRMO. 52
Figure 59. Location of geocoded photos by filename north at San Antonio. Geographic coordinates and photos are provided on the Data CD. Backdrop is an unrectified 2003 IKONOS satellite image provided by CRMO. 53
Figure 60. Location of geocoded photos by filename south of San Antonio. Geographic coordinates and photos are provided on the Data CD. Backdrop is an unrectified 2003 IKONOS satellite image provided by CRMO. 53
Figure 61. Sample statistics and grain size distribution for the beach sediment sample taken at San Antonio. 54
Figure 62. Sample statistics and grain size distribution for the beach sediment sample taken at Sugar Dock. 55
Figure 63. Sample statistics and grain size distribution for the beach sediment sample taken at Managaha Island. 56
Figure 64. Sample statistics and grain size distribution for the beach sediment sample taken at Memorial Park. 57
Figure 65. Percentage abundance of major components of the beach sediment samples. 58
Figure 66. Snapshot of the model showing the current speed and direction (depicted by colour banding and size and direction of vectors) of the surface layer in the northern lagoon at spring high tide. Note that water enters the lagoon over the reef crest, with current speeds exceeding 50 cm/s in the lagoon and a general flow to the southwest. 59
Figure 67. Snapshot of the model showing the current speed and direction (depicted by colour banding and size and direction of vectors) of the surface water layer in the northern lagoon at spring low tide. Note that the barrier reef is shown as partially dry (grey colour) and that current speeds are low (<20 cm/s), with indications of the presence of gyres within the lagoon. 59
Figure 68. Calibration results showing good agreement between water levels as derived from the model (markers) and those observed by the tide gauge (continuous line). The mean range for Saipan is 0.45 m (the difference in height between mean high water and mean low water). The diurnal range (the difference in height between mean higher high water and mean lower low water) is 0.67 m. 60
Figure 69. Calibration results showing good agreement between the observed current speed (line) of the surface layer (top panel), mid water layer (centre panel), and near-bed layer (bottom panel), and those obtained from the model (crosses) for the ADP location in the channel. 61
Figure 70. Calibration results showing good agreement between the observed current directions (line) of the surface layer (top panel), mid water layer (central panel), and near-bed layer (bottom panel), and those obtained from the model (crosses) for the ADP location in the channel. 62

List of Tables

Table 1. Current Profiler Instrument Summary 12
Table 2. Current Profiler Deployment summary 12
Table 3. Current Profiler Instrument Settings 13
Table 4. Current Profiler Velocity Data Processing 14

Table 5. Wave Gauge Instrument Summary 15
Table 6. Wave Gauge Deployment Summary 15
Table 7. Wave Gauge Instrument Settings 16
Table 8. Sediment Sample Summary 21
Table 9. Statistics for depth-averaged velocity from instrument ADP channel 29
Table 10. Statistics for depth-averaged velocity at location ADP lagoon 30
Table 11. Statistics for depth-averaged velocity from instrument AWAC outfall 35
Table 12. Monthly summary statistics for the ERA-interim wave data 42
Table 13. Tide gauge datums relative to mean sea level (source: tidesandcurrents.noaa.gov) 47
Table 14. Photo mapping summary 49
Table 15. Sand Composition Analysis (percentage abundance) 57

Acknowledgements

The successful conduct of this survey has been with the assistance of a number of individuals from CRMO and beyond. We would like to acknowledge the support of the following people: John John Sannicolas, Annie Agutto, Julie Duenas, Ben Cabrera, John Iguel, Rita Dela Cruz, Doris Chong, Rodney Camacho, John Starmer, Heidi Yelin, and Paul Camacho.

EXECUTIVE SUMMARY

Krüger, J., Kumar, S., Damlamian, H. and Sharma, A. 2010. Oceanographic Survey, Shoreline Mapping and Preliminary Hydrodynamic Modelling Report, Saipan, Commonwealth of the Northern Mariana Islands. *SOPAC Data Release Report 26*. Pacific Islands Applied Geoscience Commission: Suva, Fiji, 61 p.

The Pacific Islands Applied Geoscience Commission (SOPAC) carried out an oceanographic and shoreline mapping survey of Saipan Lagoon from April to June 2010 with the objective to establish a numerical model describing the water flow in the lagoon and to undertake a coastal erosion assessment

Current velocities (speed and direction of water flow) were measured *in situ* using three Sontek Acoustic Doppler Current Profilers (ADPs), one Nortek Acoustic Wave and Current Meter (AWAC), and one Sontek Acoustic Doppler Velocimeter (ADV). Data from the ADP at the channel show that the flow of water is predominantly out of the lagoon at a mean speed of 13 cm/s, while data from the ADP in the lagoon show that the flow of water is predominantly to the southwest at a mean speed of 10 cm/s. The ADV shows that the current direction at Managaha Island is due south at slow magnitudes of 5 cm/s while the AWAC near the Sadog Tasi outfall shows water flow is approximately 3 cm/s in an ESE direction

Surface wave parameters and water elevation were measured *in situ* using four RBR Tide and Wave Recorders, TWR-2050P, pressure sensors. The TWR on the northern reef slope recorded wave heights between 0.5 to 0.8 m, with the majority of waves having a period of 8 s, while the northern reef flat TWR shows that wave height and period are strongly modulated by the tide. The TWR on the southern reef slope recorded wave heights of generally 0.2 m with a period of 8 s, while at the reef flat wave height, period, and temperature are strongly modulated by the tide with wave periods distinctly bi-model with periods grouped at either less than 1 s or 5 s.

A Trimble R8 Global Navigation Satellite System (GNSS) was used to conduct reef and shoreline surveys. The mean height of the points collected along the reef crest was 0.51 m below the Northern Marianas Vertical Datum of 2003 (standard deviation of 0.12, minimum of -1.12 m and maximum of 0.09 m).

A handheld Garmin and Olympus digital camera were used to produce geocoded photographs of the shoreline at Managaha Island, Puntan Muchot, Sugar Dock, and San Antonio. A total of 326 geocoded photos were produced providing a detailed record of the state of shoreline along Managaha Island, Puntan Muchot, Sugar Dock, and San Antonio.

The bottom material sampling was made at four points taken from the beach at San Antonio, Sugar Dock, Managaha Island and Memorial Park. All sediment samples comprised gravely sand with an average mean grain size of 0.8 mm. The samples taken from the northern part of the lagoon, namely Managaha Island and Puntan Muchot (Memorial Park), show a high abundance (approximately 75%) of coral fragments, whereas the samples taken at Sugar Dock and San Antonio in the south of the lagoon comprise one third each of foraminifera and coral fragments. Shell fragments and *Halimeda* were minor component in all samples.

A three-dimensional hydrodynamic model domain was set up in order to study current patterns within Saipan Lagoon. The prominent feature of a strong coupling between incident wave forcing and lagoon circulation is reproduced well in the model, however, the hydrodynamic model is still under preparation at the time of writing.

1 Introduction

This report describes an oceanographic and shoreline mapping survey of Saipan Lagoon (Figure 1) carried out by the Pacific Islands Applied Geoscience Commission (SOPAC) from April to June 2010. This work was initiated by the Coastal Resources Management Office (CRMO) of the Commonwealth of the Northern Mariana Islands (CNMI). The purpose of the project was to establish a numerical model describing the water flow in the lagoon and to undertake a coastal erosion assessment. The study supports the update of the CRMO's regulations for marine and coastal activities and the 1997 Saipan Lagoon Use Management Plan (SLUMP). Specifically, CRMO requires recommendations based on defensible scientific studies of current patterns and coastal erosion trends to update the SLUMP in order to balance economic growth with sustaining a beautiful and healthy coastal environment. Hence, the scope of work was to:

- understand current patterns within the confines of Saipan Lagoon and the effects of these patterns on coastal processes and the distribution of pollutants from Sadog Tasi Sewer Outfall and priority drainages; and

- understand and manage trends in erosion or accretion of coastal beaches at Puntan Muchot (Memorial Park), Sugar Dock, San Antonio and Managaha Island; and

- project future environmental trends so appropriate management policies may be developed before adverse impacts are experienced.

This report describes the details and results of the fieldwork undertaken from April to June 2010 (oceanographic survey and shoreline mapping), the various baselines collated for the Lagoon (bathymetry and metocean data), as well as calibration results of the three-dimensional coupled wave-current model. Further analysis and interpretation of the results will follow in a companion technical report.

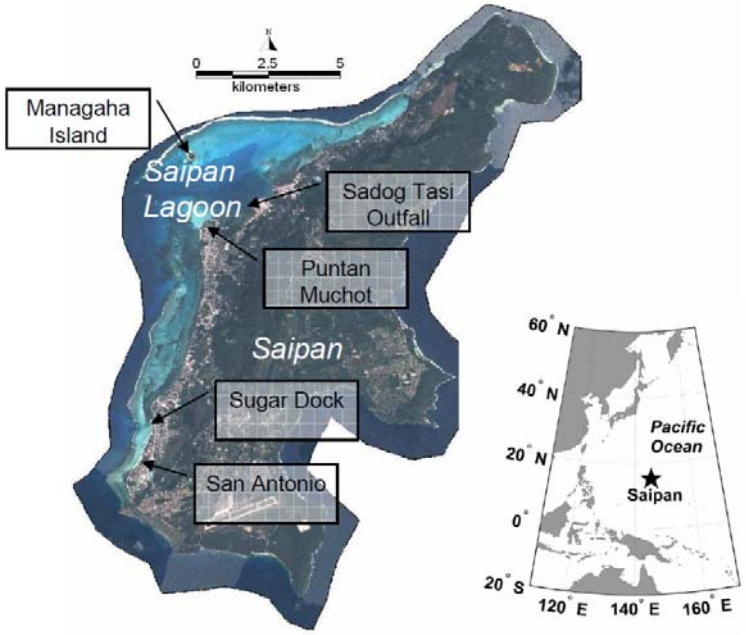

Figure 1. Map of Saipan and the location of field sites. The backdrop is an unrectified 2005 Quickbird satellite image provided by CRMO.

2 Methods

2.1 Current Meter Deployments

Current velocities (speed and direction of water flow) were measured *in situ* using three Sontek Acoustic Doppler Current Profilers (ADPs), one Nortek Acoustic Wave and Current Meter (AWAC), and one Sontek Acoustic Doppler Velocimeter (ADV). The ADPs, AWAC and ADV were deployed on the lagoon floor at the locations shown in Figure 2. The ADPs and AWAC instruments were set to measure horizontal and vertical currents throughout the water column from near bottom to near surface, whilst the ADV measured currents at a single point near the bottom. All instruments were also programmed to record water pressure and temperature at the instrument head. The ADV also measured waves.

The pressure gauges in the ADPs deployed in the channel and lagoon failed due to sediment build-up in the sensor opening. This had no effect on the instrument's ability to collect water flow data. The ADP deployed in the backreef area of the southern lagoon failed to record any data. All three instruments had to be returned to the manufacturer for repair after the survey. The AWAC and ADV functioned as expected and recorded good data. Details of the instrumental and operating parameters are listed in the tables below. A typical deployment mount is shown in Figure 3.

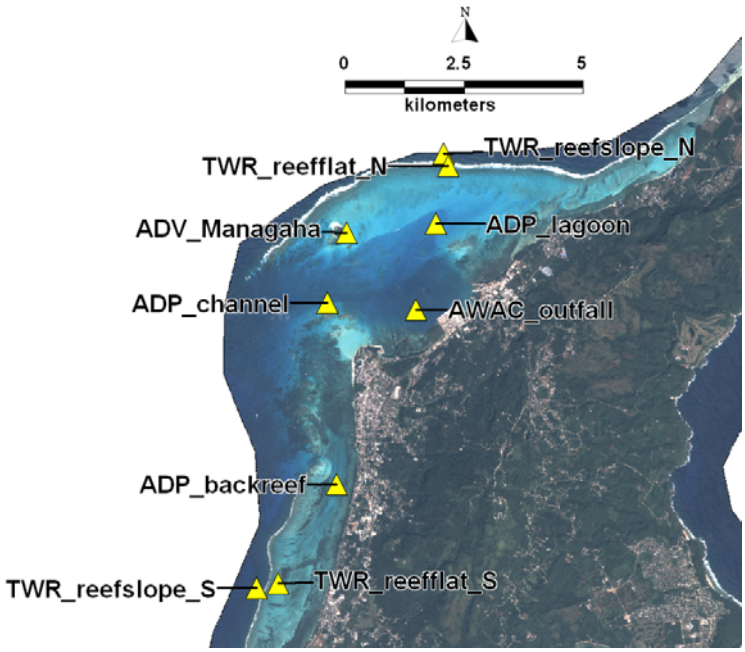

Figure 2. Mooring locations within Saipan Lagoon. Mooring stations are indicated by triangles. Background image is an unrectified 2005 Quickbird image provided by CRMO.

Figure 3. Nortek 600kHz AWAC-AST in preparation for deployment. The blue canister in the foreground is the external battery compartment. The black cylinder to the right is the acoustic release. The transducer head itself is shown sitting at the centre top of the aluminium tripod.

Table 1. Current Profiler Instrument Summary

	ADP channel	ADP lagoon	ADP backreef	ADV Managaha Is.	AWAC Outfall
Description	Acoustic Doppler Profiler	Acoustic Doppler Profiler	Acoustic Doppler Profiler	Acoustic Doppler Velocimeter	Acoustic Wave and Current Meter
Make	Sontek	Sontek	Sontek	Sontek	Nortek
Model	ADP	ADP	Mini ADP	Triton ADV	AWAC-AST
Serial No	C503	C510	M510	R053	5235
Type	Acoustic, 500 kHz	Acoustic, 500 kHz	Acoustic, 1.5 MHz	Acoustic, 10 MHz	Acoustic, 600kHz
Digital recorder	Internal	Internal	Internal	Internal	Internal
Data recorded	Velocity profiles, temperature	Velocity profiles, temperature	Velocity profiles, temperature	Velocity, temperature, waves	Velocity profiles, temperature
Comments	Pressure sensor failed	Pressure sensor failed	Instrument failed	None	None

Table 2. Current Profiler Deployment Summary

	ADP channel	ADP lagoon	ADP backreef	ADV Managaha Is.	AWAC Outfall
Location	Saipan shipping channel	Saipan lagoon	Saipan lagoon	East of Managha Island	Sadog Tasi Outfall

Table 2. Current Profiler Deployment Summary

	ADP channel	ADP lagoon	ADP backreef	ADV Managaha Is.	AWAC Outfall
Degrees Longitude (WGS84)	145.71036	145.73151	145.71230	145.71230	145.72774
Degrees Latitude (WGS84)	15.22774	15.24296	15.19305	15.24105	15.22648
Water depth, approx. (m)	11.0	8.0	4.0	1.0	11
Height above seabed (m)	0.35	0.35	0.35	0.48	0.90
Date, local time, number of first good sample	01/05/2010, 11:50:00, 23	02/05/2010, 13:30:00, 33	N/A	04/05/2010, 6:07:24, 14	03/05/2010, 15:10:00, 15
Date, local time, number of last good sample	11/06/2010, 11:30:00, 5925	11/06/2010, 09:30:00, 5769	N/A	07/05/2010, 10:07:24, 146	10/06/2010, 10:40:00, 5460
Duration of depoyment (days)	39	39	N/A	3	37
Raw data filename	MP_Saipan_ADP_channel_C503_20100501.ADP	MP_Saipan_ADP_lagoon_C510_20100502.ADP	N/A	MP_Saipan_ADV_MI_R053_20100504.tri	MP_Saipan_AWAC_outfall_5253_20100503.wpr

Table 3. Current Profiler Instrument Settings

	ADP channel	ADP lagoon	ADP backreef	ADV Managaha Is.	AWAC Outfall
Default temperature (°C)	Measured	Measured	N/A	Measured	Measured
Default salinity (psu)	34.5	34.5	N/A	34.5	35.0
Sampling interval (s)	Max. rate	Max. rate	N/A	2 Hz for waves, max. rate for currents	1 Hz
No. of samples / bursts	N/A	N/A	N/A	2048 for waves	N/A
Averaging interval (s)	180	180	N/A	180 for currents	120
Record interval (s)	600	600	N/A	1800 for both currents and waves	600

Table 3. Current Profiler Instrument Settings

	ADP channel	ADP lagoon	ADP backreef	ADV Managaha Is.	AWAC Outfall
Number of cells in profile	16	16	N/A	1	20
Blanking distance (m)	1	1	N/A	N/A	1.05
Cell size (m)	1	1	N/A	N/A	1

The raw binary files from the instruments were loaded into the Sontek ViewADP Pro v4.03, Nortek software AWAC AST v1.36, or Sontek Triton Data Post-Processing PRO v1.74c, in case of the ADPs, AWAC, and ADV, respectively, and processed using the settings listed in the table below. The raw data were then exported to readable ASCII listings and a Matlab script was used to plot the data as shown in the Results section of this report. All files are provided on the Data CD.

Table 4. Current Profiler Velocity Data Processing

	ADP channel	ADP lagoon	ADP backreef	ADV Managaha Is.	AWAC Outfall
First good cell number	1	1	N/A	N/A	1
Last good cell number	8	6	N/A	N/A	7
Salinity (psu)	34.5	34.5	N/A	34.5	35.0
Magnetic declination (deg)*	0.95	0.95	N/A	0.95	0.95
Sample averaging	Depth averaged	Depth averaged	N/A	N/A	Depth averaged

*Magnetic declination was obtained from the NOAA website: http://www.ngdc.noaa.gov/geomagmodels/Declination.jsp (accessed 16/06/2010).

2.2 Wave Gauge Deployments

Surface wave parameters and water elevation were measured *in situ* using four RBR Tide and Wave Recorders TWR-2050P pressure sensors. The TWRs were deployed in sets of two, with one on the reef slope, and the other further inshore on the reef flat (see Figure 2 for locations). Details of the instrument settings are shown in the tables below. A typical deployment mount is shown in Figure 4.

Figure 4. The tide and wave recorder RBR-TWR-2050P (26.5 cm x 3.8 cm overall dimensions) was contained within the protective PVC housing, attached to an aluminium frame, and weighed down with scrap metal, before being placed on the seabed.

Table 5. Wave Gauge Instrument Summary

	TWR, Reef Slope, North	TWR Reef Flat, North	TWR, Reef Slope, South	TWR Reef Flat, South
Description	Tide and Wave Recorder	Tide and Wave Recorder	Tide and Wave Recorder	Tide and Wave Recorder
Make	RBR	RBR	RBR	RBR
Model	TWR-2050P	TWR-2050P	TWR-2050P	TWR-2050P
Serial No	15483	15486	15484	15485
Type	Pressure sensor	Pressure sensor	Pressure sensor	Pressure sensor
Digital recorder	Internal	Internal	Internal	Internal
Data recorded	Tides, temperature, waves	Tides, temperature, waves	Tides, temperature, waves	Tides, temperature, waves
Comments	None	None	None	None

Table 6. Wave Gauge Deployment Summary

	TWR, Reef Slope, North	TWR Reef Flat, North	TWR, Reef Slope, South	TWR Reef Flat, South
Degrees Longitude (WGS84)	145.73300	145.73387	145.69676	145.70091
Degrees Latitude (WGS84)	15.25622	15.25387	15.17324	15.17410

Table 6. Wave Gauge Deployment Summary				
	TWR, Reef Slope, North	TWR Reef Flat, North	TWR, Reef Slope, South	TWR Reef Flat, South
Water depth, approx. (m)	15	1	13	1
Height above seabed (m)	0.5	0.5	0.5	0.5
Date, local time, number of first good sample	29/04/2010, 10:50:00, 3	29/04/2010, 15:50:00, 8	30/04/2010, 10:50:00, 3	30/04/2010, 11:50:00, 4
Date, local time, number of last good sample	09/06/2010, 13:50:00, 990	10/06/2010, 11:50:00, 1012	09/06/2010, 14:50:00, 967	15/06/2010, 09:50:00, 1106
Duration of depoyment (days)	40	41	39	45
Filename	MP_Saipan_TWR_reefslope_N_15483_20100429.hex	MP_Saipan_TWR_reefflat_N_15486_20100429.hex	MP_Saipan_TWR_reefslope_S_15484_20100430.hex	MP_Saipan_TWR_reefflat_S_15485_20100430.hex

Table 7. Wave Gauge Instrument Settings				
	TWR, Reef Slope, North	TWR Reef Flat, North	TWR, Reef Slope, South	TWR Reef Flat, South
Default temperature (°C)	Measured	Measured	Measured	Measured
Default salinity (psu)	N/A	N/A	N/A	N/A
Sampling interval (s)	2 Hz	2 Hz	2 Hz	2 Hz
No. of samples/bursts	2048 for waves	2048 for waves	2048 for waves	2048 for waves
Averaging interval (s)	180 for tides	180 for tides	180 for tides	180 for tides
Record interval (s)	3600 for waves and 600 for tides	3600 for waves and 600 for tides	3600 for waves and 600 for tides	3600 for waves and 600 for tides

The raw data (.hex file) were downloaded from the instruments and exported from the RBR software Ruskin v.3.1 to readable ASCII listings. The data files are provided on the Data CD. A Matlab script was used to generate plots from these data as shown in the Results section of this report.

2.3 GNSS Reef and Shoreline Survey

A Trimble R8 Global Navigation Satellite System (GNSS) was used to conduct reef and shoreline surveys during the field visit in May 2010. In addition to the designated field sites, a section of the barrier reef crest was also surveyed. Wave climate data showed that ocean surface waves predominantly arrive from the east northeast (see the Results

Section on ECMWF data below). Preliminary wave modelling and visual inspection of satellite imagery also showed that the waves refract around the island of Saipan and align themselves with an east-west trending section of the barrier reef to the northeast of Managaha Island. This four kilometre long section of the reef was therefore assumed to be the most energetic part of the reef complex, and accurate height information of the reef was deemed to be important for modelling purposes. This section of the barrier reef was therefore included in the GNSS survey along with the shoreline survey of the upper beach and toe of the beach at the focal areas of Managaha Island, Puntan Muchot, Sugar Dock, and San Antonio (see Figure 5 for locations).

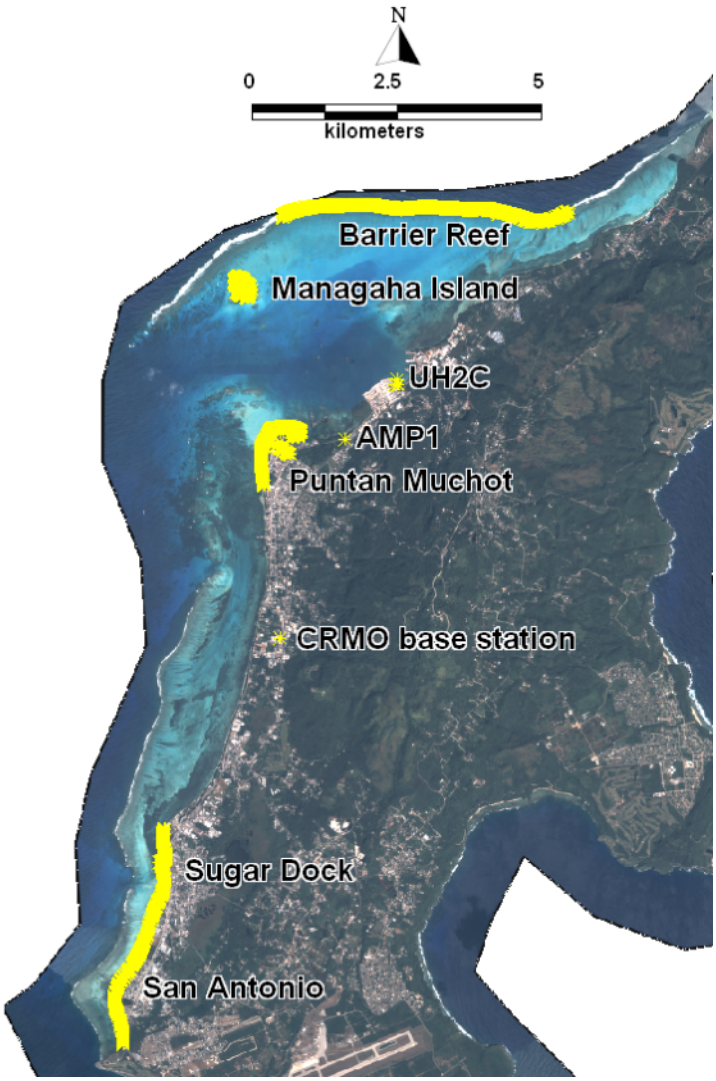

Figure 5. GNSS survey points. Base stations were set up at the CRMO office building and the University of Hawaii tide gauge survey mark UH2C, which provided vertical control for the survey. Backdrop is an unrectified 2005 Quickbird image supplied by CRMO.

The system was operated in a Post-Processing Kinematic (PPK) mode, which involved two roving receivers and one reference receiver that remained stationary over a known control point. GNSS data were then simultaneously collected at the reference and rover receivers during the survey operation. The reference station was set up on the roof of the CRMO building and set to log epochs in a static survey mode (see Figure 6). The rovers were attached to 2 m long survey poles and used in a stop and go survey mode logging 5 epochs at each point of interest.

One rover was used to map the upper beach and the second was used to map the toe of the beach as shown in Figure 7. The upper beach was depicted as the seaward berm or scarp. If these features were not distinct, the outer edge of the vegetation was mapped.

The toe of the beach was depicted as the point where the sand beach slope intersects the more horizontal lagoon floor.

Figure 6. Base station on the southwest corner of the flat-topped building of the CRMO office. The unit was levelled on top of an existing timber bar attached to the roof with a nail at its centre (see inset).

Figure 7. The two rovers mounted on 2 m survey poles during the shoreline survey at Memorial Park. One receiver can be seen at the vegetated berm to the left, and the other being held by the surveyor at the toe of the beach.

The Northern Marianas Vertical Datum of 2003 (NMVD03) is the official civilian vertical datum for surveying and mapping activities. It is defined as Mean Sea Level from water level observations spanning the period 1983-2001 at the National Water Levels Observation Network bench mark number 163 3227 UH-2C (1.657 meters), located at Tanapag Harbour (Department of Commerce, 2009). Vertical control for the reef and shoreline survey was therefore provided by observing the tide gauge bench mark for six hours while simultaneously logging GNSS epochs at the CRMO base station (Figure 8).

Figure 8. Tripod and Trimble R8 receiver set up over the tide gauge bench mark at Tanapag Harbour. Observing the tide gauge bench mark provided control for the survey and ensured that post-processed heights were relative to NMVD03. The tide gauge can be seen immediately behind and above the tripod. See Figure 11 for location.

The stop and go PPK method of surveying was chosen as this procedure is very productive and produces the largest number of survey points in the least amount of time. However, the relatively long baselines (maximum distance from the rovers to the base station was 9 km) and the shortened occupation times (five epochs in the case of this survey), resulted in the degradation of horizontal and vertical accuracies of the survey points. Another contributing factor was the difficulty to steady the survey pole in the surf zone, in the case of the reef survey, or to keep it level in the soft sand during the beach survey. The proximity of large trees along the shoreline may have also obscured a number of satellites, making the observations more ambiguous. The acceptance criteria for processed points were 0.400 m + 1.0 ppm in the horizontal and 0.500 m + 1.0 ppm in the vertical. The processing was done using the Trimble Business Center software v1.11.

2.4 GPS Photo Shoreline Mapping

A handheld Garmin Vista HCx GPS and Olympus digital camera were used to produce geocoded photographs of the shoreline at Managaha Island, Puntan Muchot, Sugar Dock, and San Antonio. At the beginning of each survey the GPS was set to log position and time at five second intervals, and a photo was taken of the display of the GPS showing the time of day (Figure 9). This effectively synchronised the respective internal clocks in the GPS and the camera for post-processing. The procedure then involved carrying the handheld GPS around the neck while taking photos of the shoreline.

Figure 9. A photo was taken of the handheld GPS displaying the time of day in local standard time at the start of each survey. This enabled geocoding of any subsequent photos by way of matching the GPS location and time with the time stamp embedded in the EXIF information of the JPEG photo file.

At the end of the survey the track log from the GPS (.gpx file) was saved along with the digital photos downloaded from the camera. The open source software GPicSync v1.28 (http://code.google.com/p/gpicsync/) was then used to geocode the photos by tagging each photo with the appropriate geographic coordinates from the GPX file using time as the common reference. GPicSync also had the option of generating KML and KMZ files for use in Google Earth (see Figure 53 in the Results section). In combination, the digital camera and GPS gave a permanent record of the shoreline in time and space.

2.5 Sediment sampling

The bottom material sampling was made at four points taken from the beach at San Antonio, Sugar Dock, Managaha Island and Memorial Park (see Figure 10 and table below for locations). The objective of the sediment sampling was to analyse the sediments from different locations within the lagoon for grading structure and to compare major composition ratios (corals, foraminifera, *Halimeda*, and shell pieces).

Figure 10. Beach sediment sample locations. See table below for more information. Background image is an unrectified Quickbird 2005 image supplied by CRMO.

Table 8. Sediment sample summary

Location Date	Latitude	Longitude	Sample Photo
San Antonio, 8/05/2010	15° 08' 0.66"	145° 41' 37.73"	

Table 8. Sediment sample summary

Location Date	Latitude	Longitude	Sample Photo
Sugar Dock, 8/05/2010	15° 09' 3.18"	145° 41' 59.27"	
Managaha Island, 7/05/2010	15° 14' 27.38"	145° 42' 49.39"	
Memorial Park, 6/05/2010	15° 13' 10.27"	145° 43' 16.04"	

The samples were taken by scooping a mixed sample of about 200 to 500 g of sand from the surface layer of the beach face. The position was marked by logging the position given by a handheld Garmin GPS. The samples were stored in a zip-lock bag and transported to SOPAC in Suva, Fiji, and dried in an oven at 121 degrees Celsius for 15 minutes. The dried samples were split in two, one for grain size analysis at full Phi intervals and the other for analysis of sand composition ratio under a stereo microscope. Grain size analysis was done using the GRADISTAT version 7.0 Macro for Excel (downloaded from www.kpal.co.uk, accessed July 2010). Summary statistics of this analysis are presented in the Results section below. The details of the analysis are provided on the Data CD.

The sand composition ratio was calculated by examining 100 random grains from each of the unsieved split samples, and counting the number of coral fragments, foraminifera, shell fragments, and *Halimeda* present. This was repeated three times for each sample and the average of this is reported in the Results section.

2.6 Oceanography and Meteorology

A tide gauge with the station identifier 1633227 is installed at Tanapag Harbour (Figure 11) providing water level measurements every six minutes. The observed water level data were obtained from the NOAA Tides & Currents website (http://tidesandcurrents.noaa.gov/, accessed June 2010). The Mean Sea Level observed at the tide gauge for the epoch 1983 to 2001 is the official basis for the Northern Marianas Vertical Datum of 2003 (NMVD03).

Figure 11. Location of the Saipan Tide gauge (marked by circle) within the grounds of the Port of Saipan where the east parking lot meets with the east face of Delta Dock.

Hourly meteorological data recorded at Saipan International Airport (15.1190°N, 145.7290°E, elevation 65 m) for the period from 02/05/2010 22:54:00 to 27/06/2010 21:54:00 were obtained from the internet (http://weather.gladstonefamily.net/site/PGSN, accessed June 2010). The time series consisted of the following parameters.

- Date and time, UTC
- Barometric pressure (mbar)
- Temperature (degrees F)
- Dewpoint (degrees F)
- Relative humidity (%)
- Wind speed (mph)
- Wind direction (degrees)

Global metocean model data were obtained from the ERA-interim website of the European Center for Medium-Term Weather Forecasting (ECMWF, data-portal.ecmwf.int/data/d/interim_daily/, accessed 24 June 2009), spanning the time period from 01/01/1989 to 30/04/2009. Details of the model can be found in ECMWF (2007). A Matlab script was used to extract a time series for a model point approximately 100 km northeast of Saipan (Figure 2) from the global ERA-interim NetCDF files. The model point immediately west of Saipan was not used in order to avoid possible interference of the land mass. The time series consisted of the following parameters:

- Date and time in UTC
- Hs, significant wave height (m)
- Tm, mean wave period (s)
- Dm, mean wave direction (degrees, meteorological convention)

- U10, 10 m U wind component (m^{-s})
- V10, 10 m V wind component (m^{-s})
- Pm, mean sea level pressure (Pa)

This data was imported into the Matlab software environment for plotting and calculation of basic statistical parameters as given in the Results section of this report.

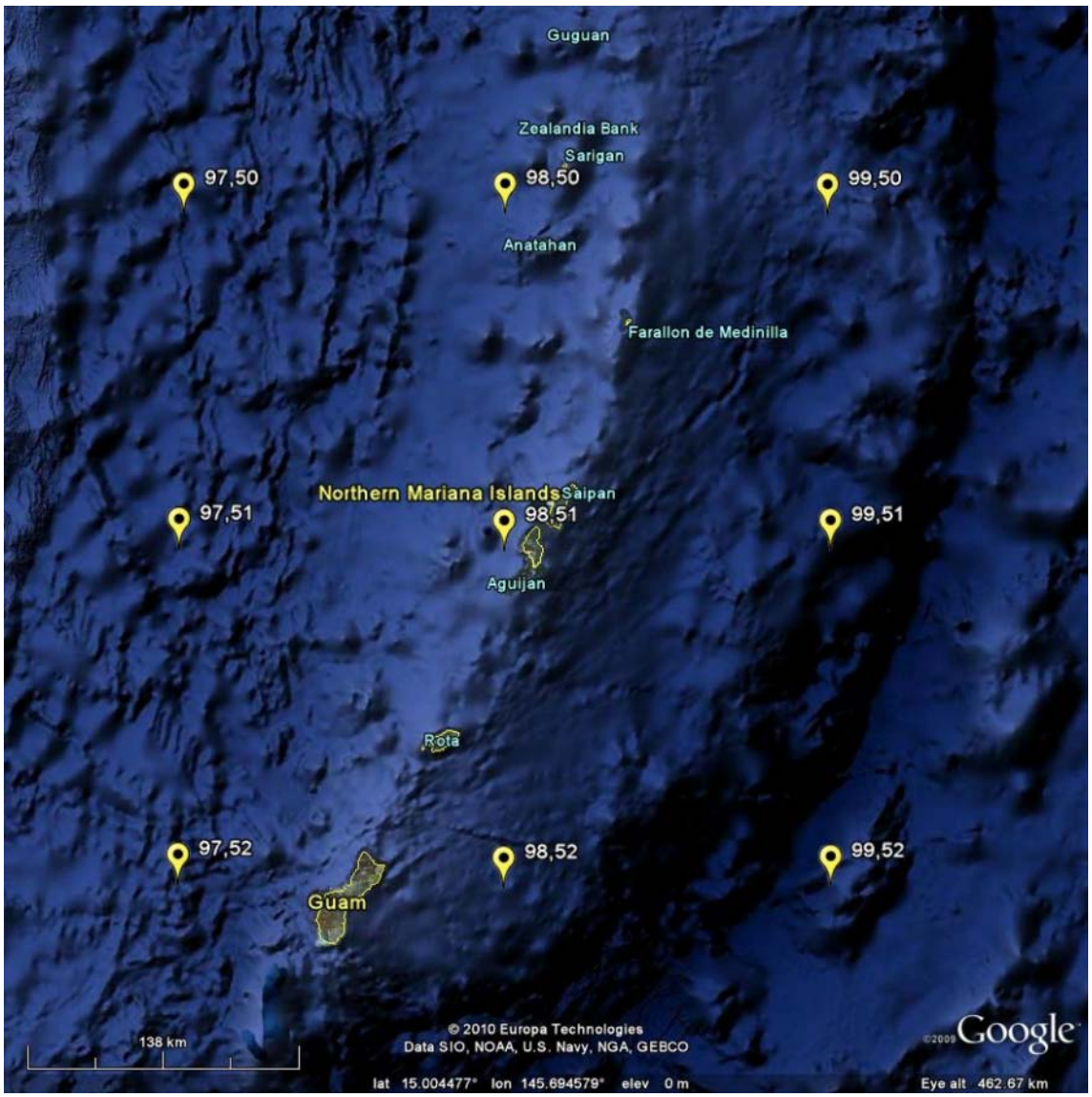

Figure 12: ECMWF ERA-Interim model data points near Saipan. A 20-year time series of met-ocean data was extracted for grid point 99,50 northeast of Saipan at 147.0°E 16.5°S (position marked by the upper right hand corner balloon).

2.7 Wave-Current Hydrodynamic Model

A three-dimensional hydrodynamic model domain was set up in order to study current patterns within Saipan Lagoon. The water circulation in Saipan lagoon is influenced by an interplay of tides, winds and incident ocean waves, and each of these forces were accounted for in the model.

The model domain was constructed using a combination of triangular and quadrangular meshes over gridded bathymetry obtained from the Pacific Island Benthic Habitat Mapping Centre, PIBHMC (www.soest.hawaii.edu/pibhmc/, accessed June 2010). This

bathymetry is shown in Figure 13, comprising merged depth data from Multibeam and LIDAR surveys as well as satellite-derived depths to achieve full coverage over the lagoon area. The resultant domains for the wave and hydrodynamic model are shown in Figure 15 and Figure 16, respectively.

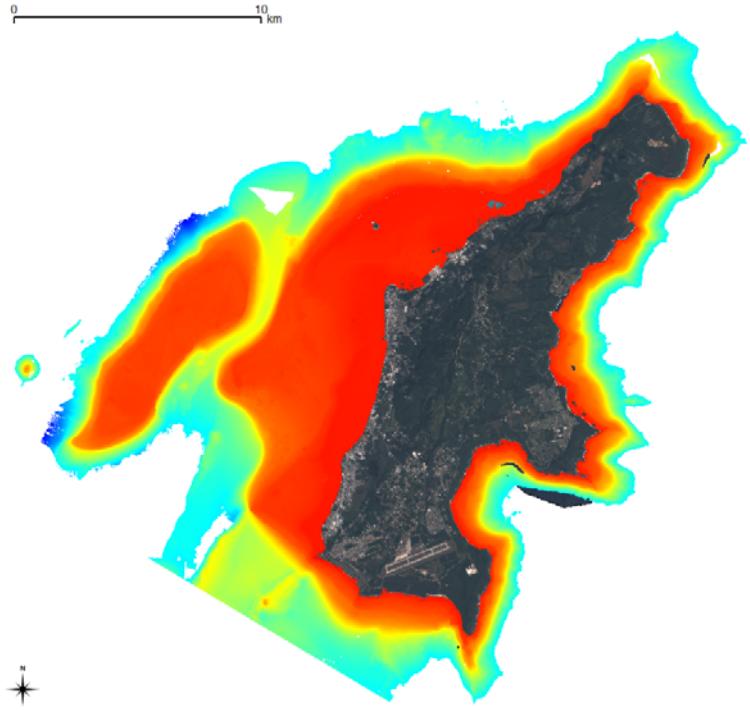

Figure 13. Composite bathymetry for Saipan Island, shallow to deep waters (0 to 600 m) are shown as red to blue. This 5 m grid obtained from PIBHMC formed the basis of the bathymetry data for the hydrodynamic model.

However, upon closer inspection it was found that the PIBHMC dataset contained questionable values for the shallowest depths along the reef crest (Figure 14). It is assumed that this high energy environment could not be mapped by any of the applied techniques (multibeam, LIDAR or satellite-derived). The identified problem areas were filled by assuming that the reef reaches a height of mean lower-low water or 0.392 m below mean sea level as defined by the NMVD03 (also refer to the Results Section of the GNSS survey).

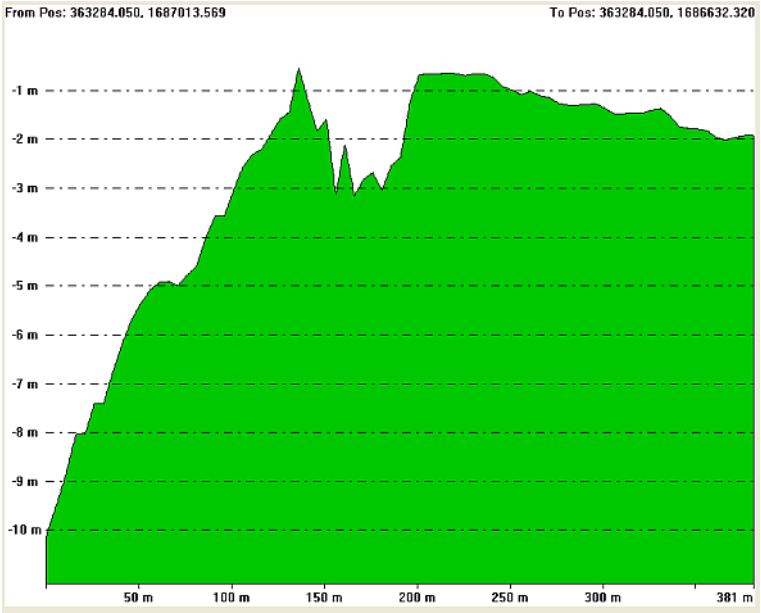

Figure 14. An approximately 400 m long representative cross-section perpendicular to the barrier reef north of Managaha Island from the merged dataset obtained from PIBHMC. Note that the plot shows erroneous depths of approximately 3 m below datum along a 50 m section over the shallowest part of the reef. This reef crest area was replaced with depth values of -0.392 m (MLLW) below mean sea level in the model domain.

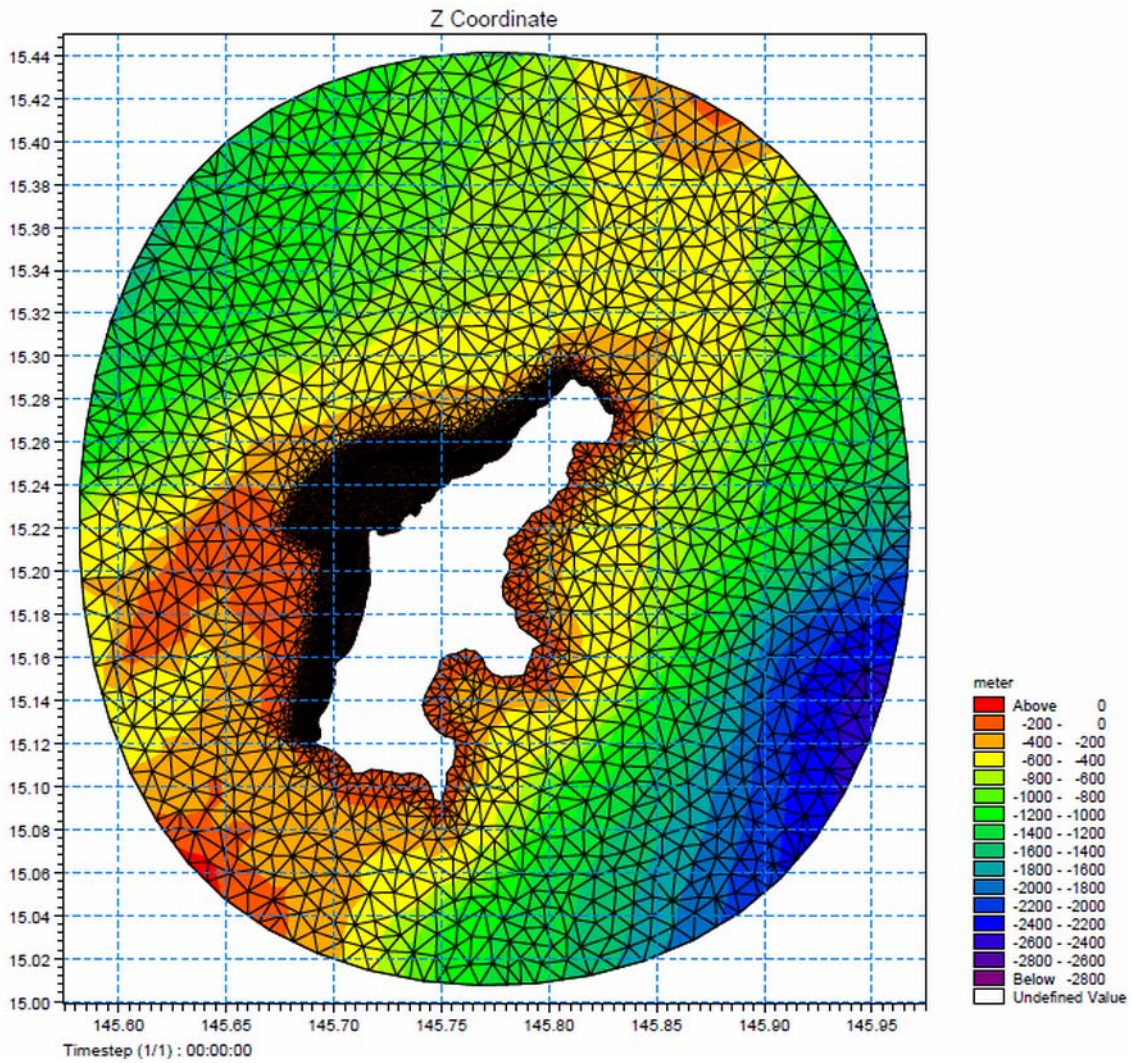

Figure 15. Mesh grid of the wave model domain. Shallow to deep waters (0 to below 2800 m) are shown as red to purple.

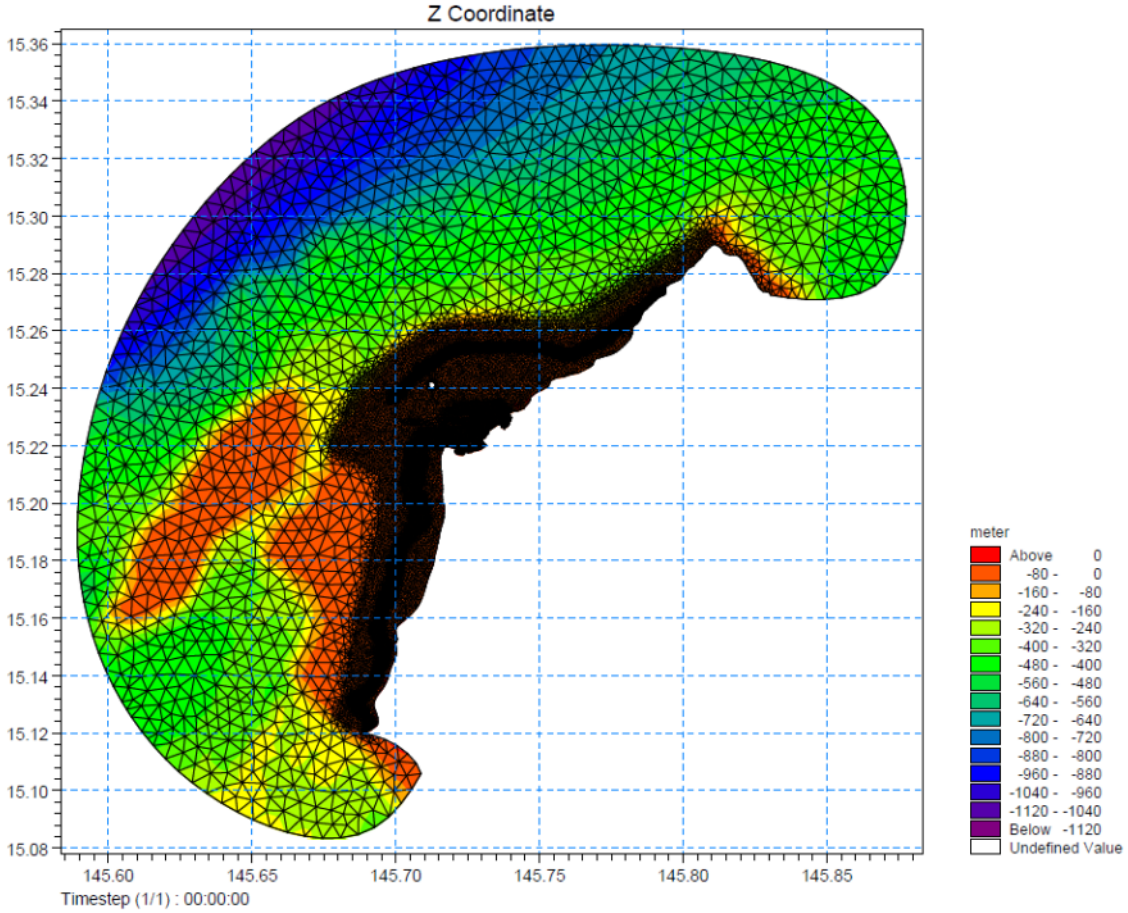

Figure 16. Mesh grid of the hydrodynamic model domain. See Figure 17 for details of the Harbour area. Shallow to deep waters (0 to below 1120 m) are shown as red to purple.

A quadrangular mesh was used to depict the dredged navigational channel in order to satisfy the channel's geometry. Finer unstructured meshes were created over the forereef slopes, reef crests, and reef flats, to better resolve the morphology of the barrier reef and account for wave set-up and wave induced current (see Figure 17).

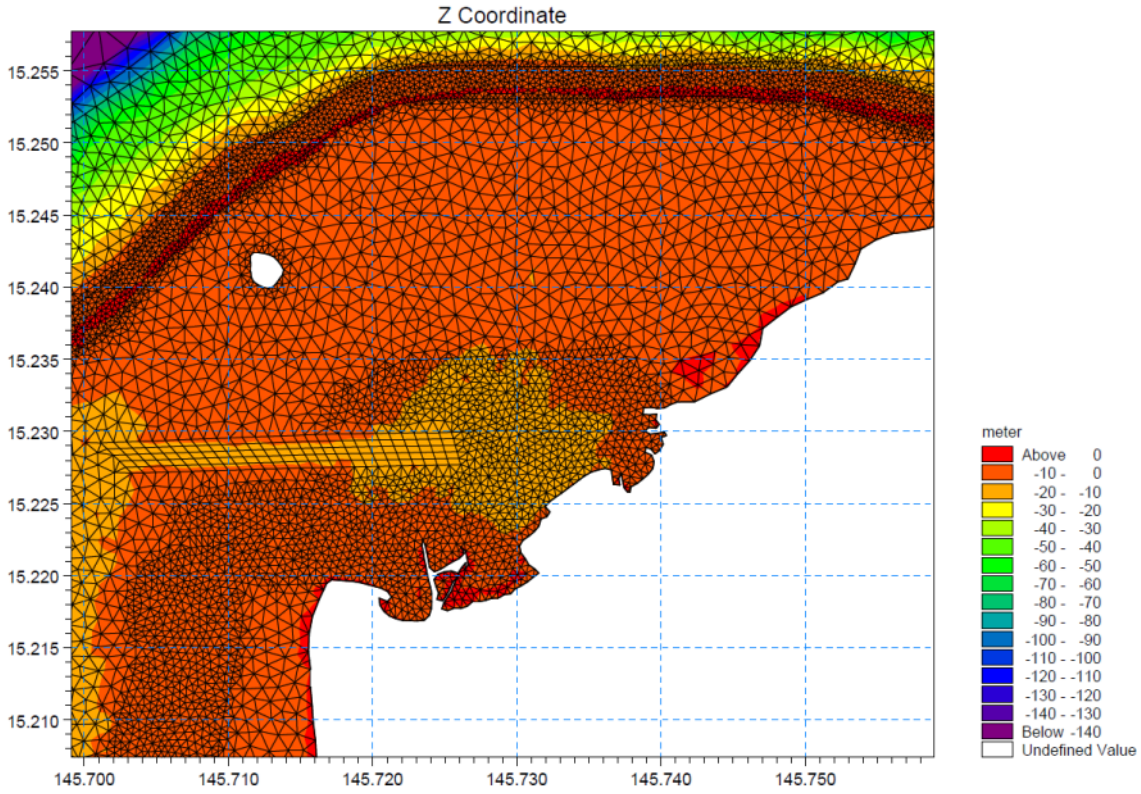

Figure 17. Detail of the hydrodynamic model domain over the northern Saipan Lagoon area. The navigational channel is resolved using a quadrangular mesh and can be seen to the middle left of the image. Mesh size was smallest over the barrier reef depicted by the band along the top of the image, where the maximum length of a mesh segment was constrained to 35 m. Shallow to deep waters (0 to below 140 m) are shown as the colour band from red to purple.

The wave model was calibrated against the collected wave data, namely, significant wave height (Hs), wave period (Tp), and water level. A time series of radiation stress (Sxx, Sxy, Syy) was extracted from each node of the wave model and included in the hydrodynamic model to account for wave forcing. The resultant hydrodynamic model was calibrated against field data of current speed and direction from the ADPs and AWAC, as well as water level data from the tide gauge and pressure sensors (TWRs). The calibration results as shown in the Results section of this report.

The model will be used to analyse the dynamics of current patterns within the lagoon under seasonal as well as inter-annual met-ocean conditions. This will provide a better understanding of the physical processes in the lagoon and their influence on the advection and dispersion of pollutants from the Sadog Tasi outfall, while residual current vectors will provide information on the dominant sediment transport directions. These studies will form part of the companion technical report.

3 Results

3.1 ADP Channel

Water flow observations made by the ADP in the channel (see Figure 2 for locations) are summarised in the table below. Time series and bivariate plots of depth averaged current speeds and direction are shown in the subsequent plots. The data show that the flow of water is predominantly out of the lagoon at a mean speed of 13 cm/s. Maximum speeds of 40 cm/s or more were observed on three occasions that coincided with higher incident offshore wave events.

Table 9. Statistics for depth averaged velocity from instrument ADP channel	
Minimum speed (cm/s)	0.1
Maximum speed (cm/s)	46.5
Mean speed (cm/s)	13.1
Standard deviation of speed (cm/s)	9.7
Minimum direction (º)	0.3
Maximum direction (º)	359.5
Mean direction (º)	234.1
Standard deviation of direction (º)	60.0

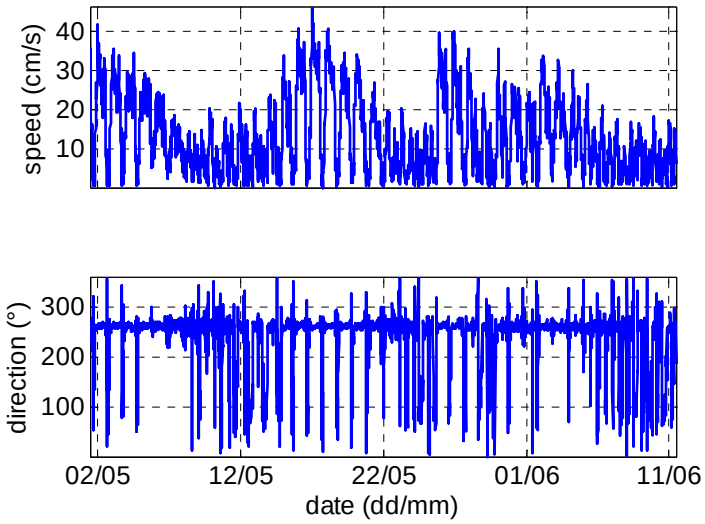

Figure 18. Time series plot of depth-averaged current speed and direction measured by the ADP in the channel. Direction is given from true north in oceanographic convention (going toward).

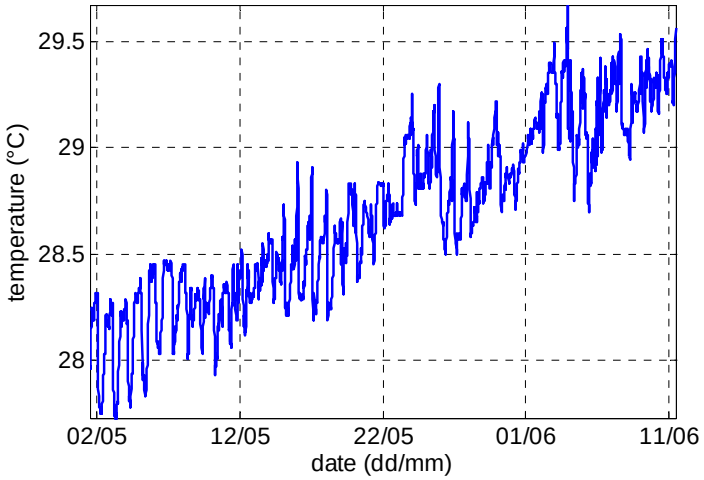

Figure 19. Time series of temperature as recorded by the ADP in the channel.

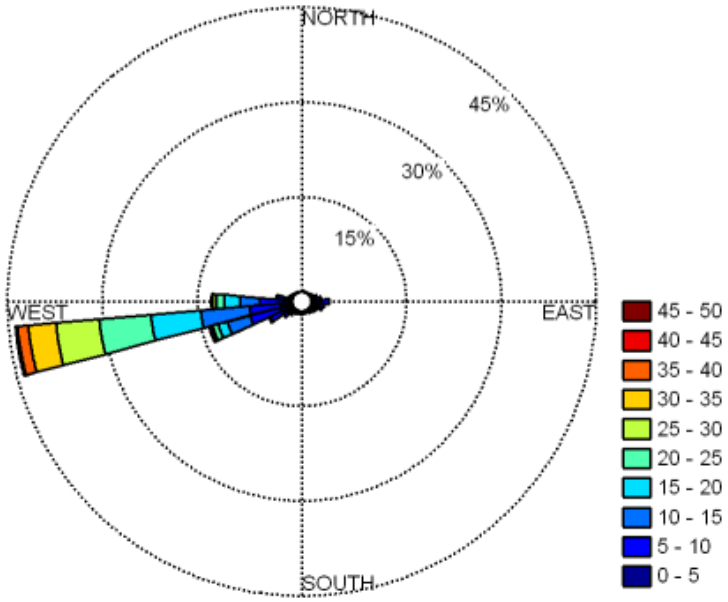

Figure 20. Current rose for depth-averaged velocities measured by the ADP in the channel. Directions are shown from true north in oceanographic convention (going toward). Current speeds are given in cm/s.

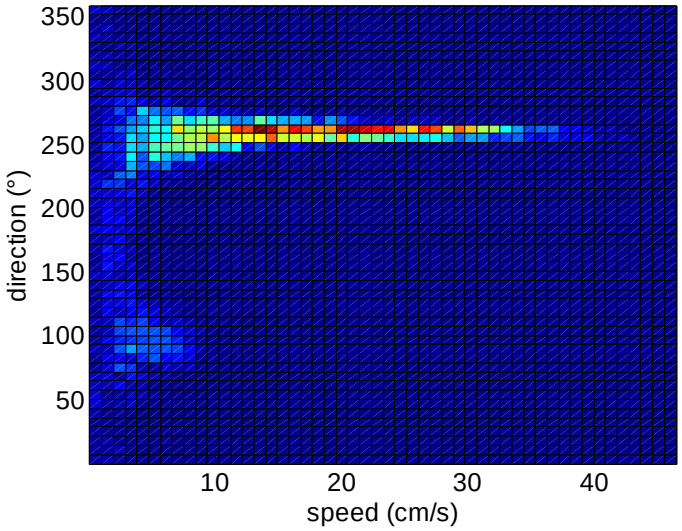

Figure 21. Scatter density plot of depth averaged current speed and direction measured by the ADP in the channel. Blue to red indicates a range from low to high occurrence of a particular bivariate combination. Direction is given from true north in oceanographic convention (going toward).

3.2 ADP Lagoon

Water flow observations made by the ADP in the lagoon (see Figure 2 for locations) are summarised in the table below. Time series and bivariate plots of depth averaged current speeds and direction are shown in subsequent figures. The data show that the flow of water is predominantly to the southwest at a mean speed of 10 cm/s. Speeds exceeding 20 cm/s and up to a maximum of 30 cm/s were observed during periods with offshore wave height of at least 1 m (refer to Figure 31). Current directions were more variable, and occasionally reversed, with flow toward the northeast at some 5 cm/s, during low tide and calm offshore conditions.

Table 10. Statistics for depth averaged velocity at location ADP lagoon	
Minimum speed (cm/s)	0.1
Maximum speed (cm/s)	30.1

Table 10. Statistics for depth averaged velocity at location ADP lagoon	
Mean speed (cm/s)	10.6
Standard deviation of speed (cm/s)	5.9
Minimum direction (º)	0.9
Maximum direction (º)	360.0
Mean direction (º)	216.7
Standard deviation of direction (º)	45.5

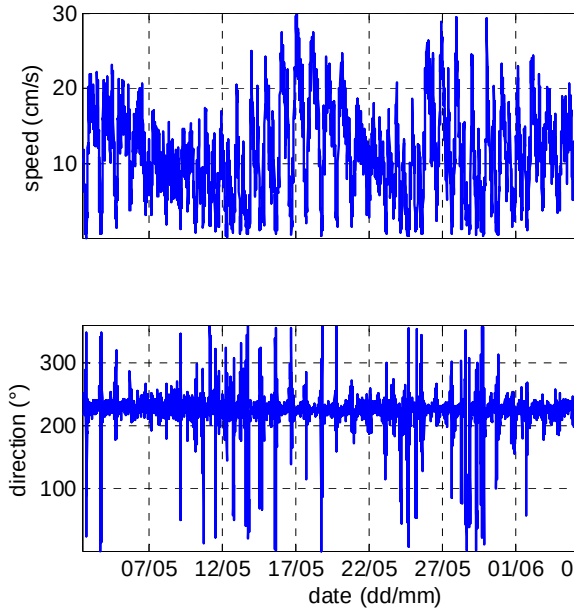

Figure 22. Time series plot of depth averaged current speed and direction measured by the ADP in the lagoon. Direction is given from true north in oceanographic convention (going toward).

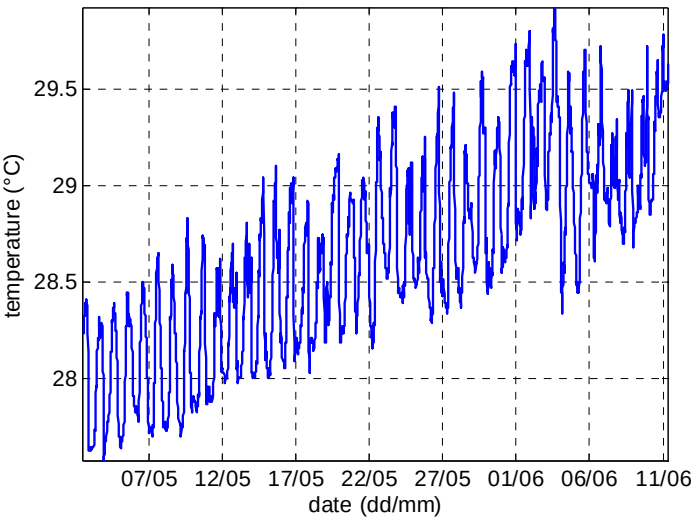

Figure 23. Time series of temperature as recorded by the ADP in the lagoon.

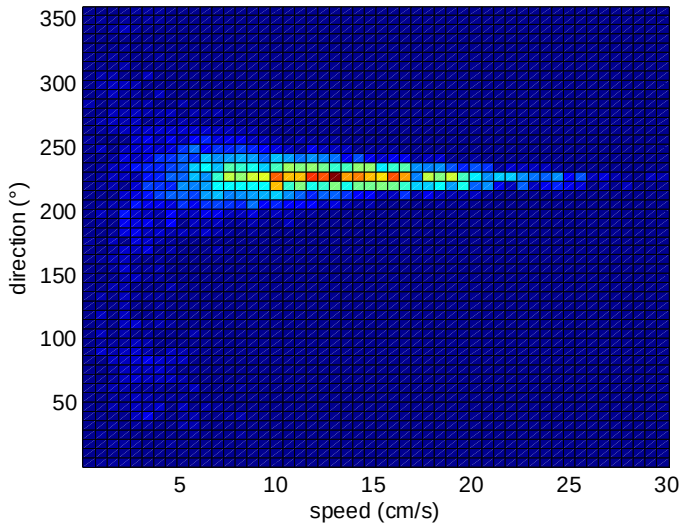

Figure 24. Scatter density plot of depth-averaged current speed and direction measured by the ADP in the lagoon. Blue to red indicates a range from low to high occurrence of a particular bivariate combination. Direction is given from true north in oceanographic convention (going toward).

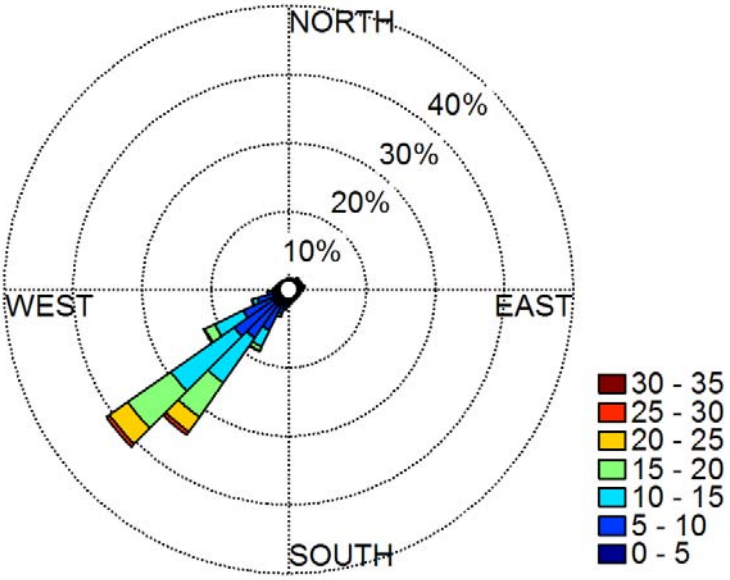

Figure 25. Current rose for depth averaged velocities (cm/s) measured by the ADP in the lagoon. Directions are shown from true north in oceanographic convention (going toward).

3.3 ADV Managaha Island

Time series plots of water velocities and wave observations made by the ADV to the east of Managaha Island are shown in Figure 26 and Figure 27, respectively. The ADV was only deployed for a duration of three days due to limitations on battery power. Current direction is due south at slow magnitudes of 5 cm/s. Wave periods and heights appear to increase with tidal heights. A wind-wave event (periods of 2 s and wave heights of 18 cm) was recorded near mid-day on 6 May.

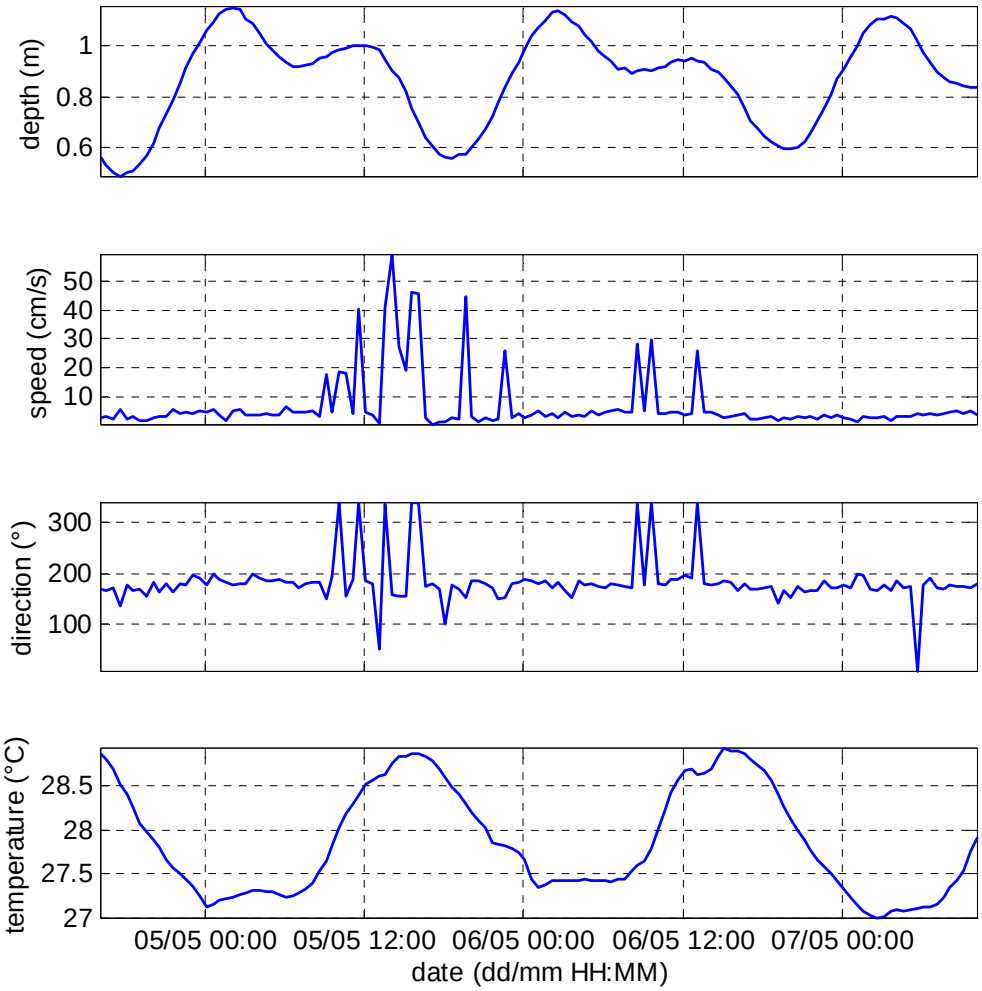

Figure 26. Time series plot of water depth, current speed, current direction, and temperature measured by the ADV at Managaha Island. Direction is given from true north in oceanographic convention (going toward).

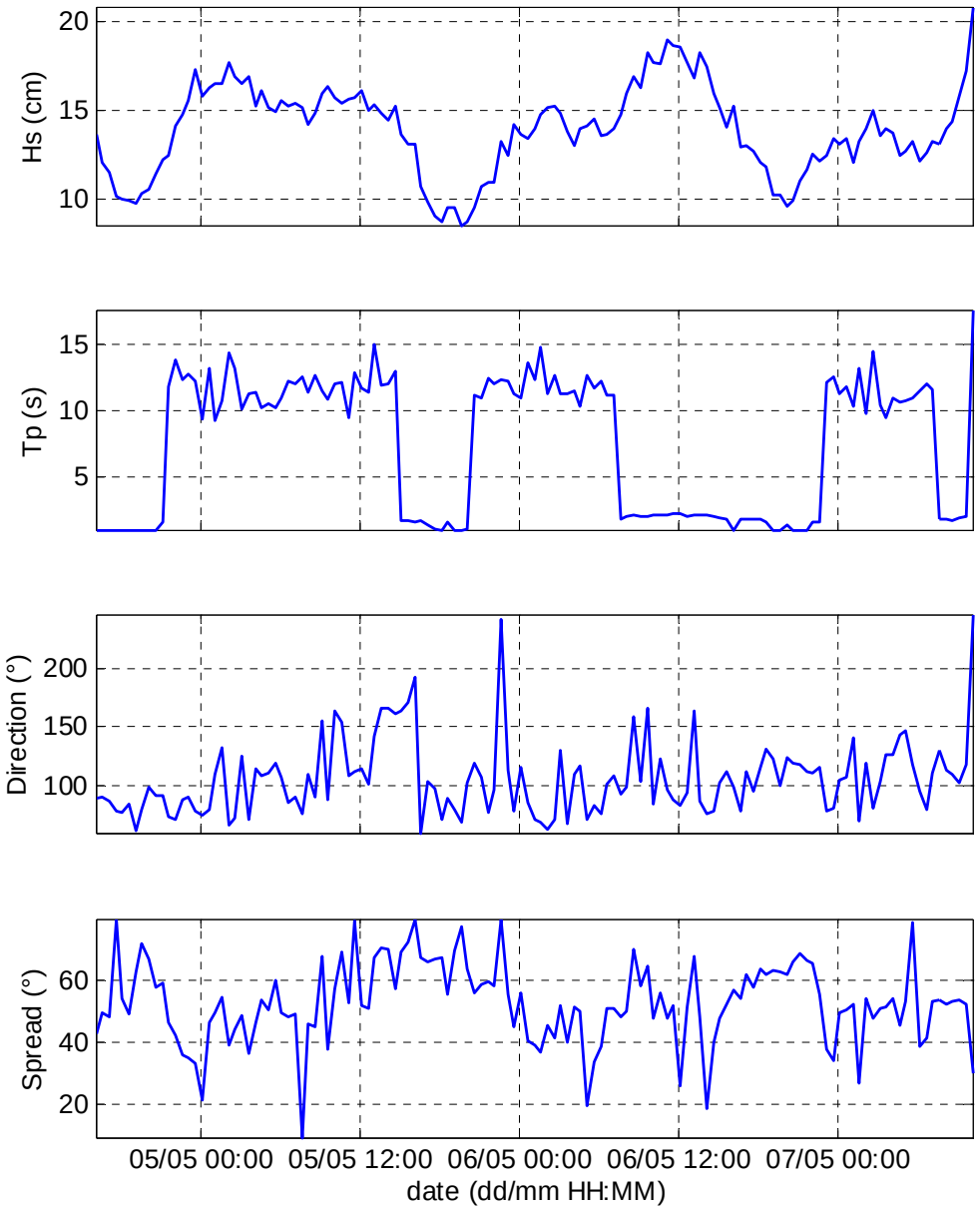

Figure 27. Time series plot of significant wave height (Hs), peak wave period (Tp), wave direction, and directional spread measured by the ADV at Managaha Island. Direction is given from true north in oceanographic convention (going toward).

3.4 AWAC Outfall

Water flow observations made by the AWAC near the Sadog Tasi outfall (see Figure 2 for locations) are summarised in the table below. Time series and bivariate plots of depth-averaged current speeds and direction are shown in subsequent figures. The plots show that the current speeds are relatively low and the direction is variable (SD of 77) when compared to the data obtained from the other current profilers. Water flow is generally at approximately 3 cm/s in an ESE direction.

Table 11. Statistics for depth averaged velocity from instrument AWAC outfall	
Minimum speed (cm/s)	0.0
Maximum speed (cm/s)	43.0
Mean speed (cm/s)	2.8
Standard deviation of speed (cm/s)	1.6
Minimum direction (º)	0
Maximum direction (º)	360
Mean direction (º)	146
Standard deviation of direction (º)	77

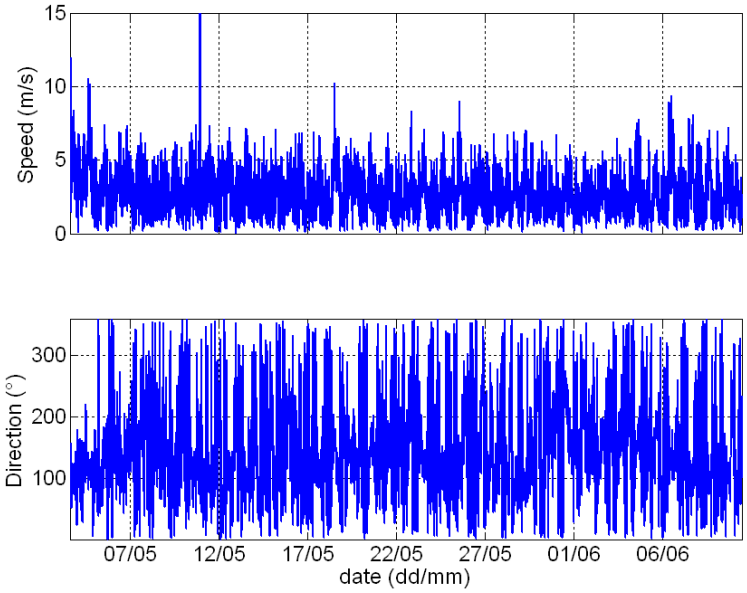

Figure 28. Time series plot of depth-averaged current speed and direction measured by the AWAC near the outfall (see Figure 2 for location). Direction is given from true north in oceanographic convention (going toward).

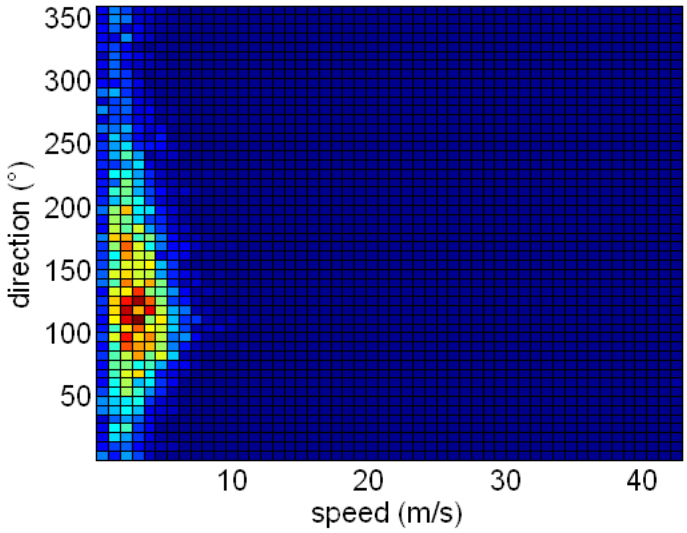

Figure 29. Scatter density plot of depth-averaged current speed and direction measured by the AWAC near the outfall. Blue to red indicates a range from low to high occurrence of a particular bivariate combination. Direction is given from true north in oceanographic convention (going to).

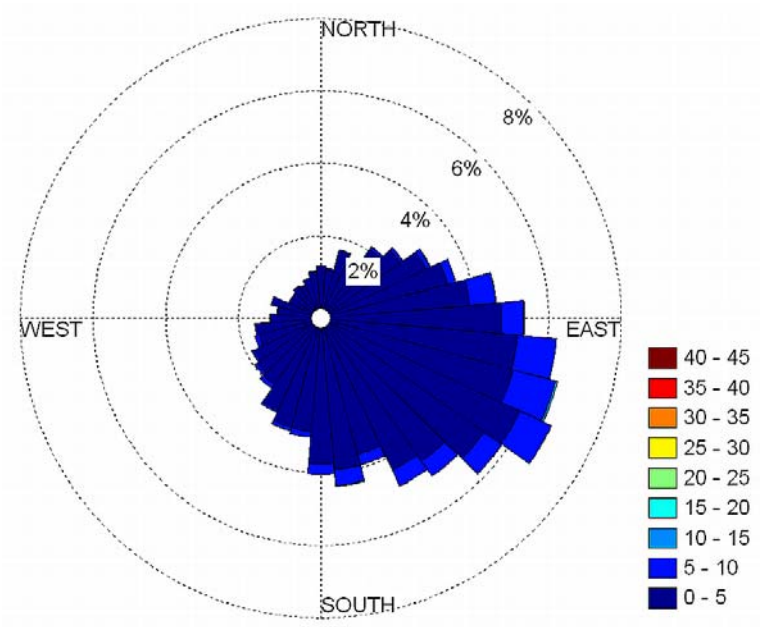

Figure 30. Current rose for depth-averaged velocities (cm/s) measured by the AWAC near the outfall. Directions are shown from true north in oceanographic convention (going toward).

3.5 TWR Reef Slope North

The TWR on the northern reef slope (see Figure 2 for location) recorded incident surface waves as well as water depth and water temperature. Time series plots of this data and a bivarate histogram of the wave period versus the wave height are shown below. Wave heights were generally between 0.5 to 0.8 m, with the majority of waves having a period of 8 s. The instrument also recorded three separate swell events reaching or exceeding wave periods of 11 s.

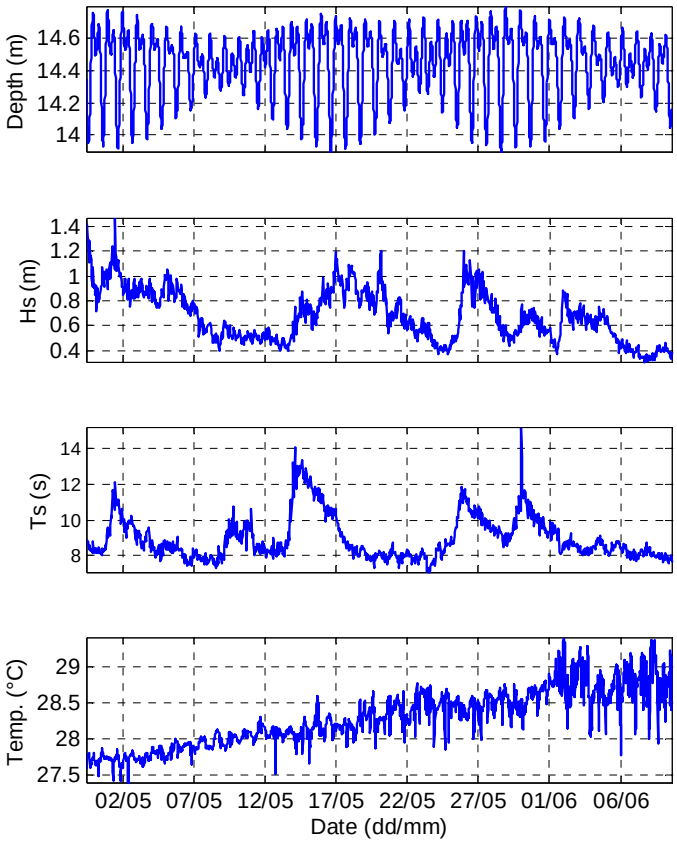

Figure 31. Time series plot of depth (m), significant wave height (Hs), significant wave period (Ts) and temperature (°C) as measured by the TWR on the northern reef slope.

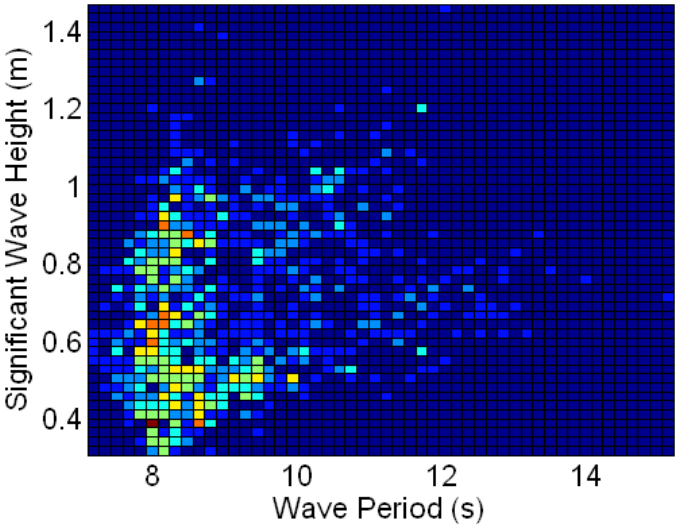

Figure 32. Scatter density plot of significant wave period and wave height for the TWR on the northern reef slope. Blue to red indicates a range from low to high occurrence of a particular bivariate combination.

3.6 TWR Reef Flat North

The TWR on the northern reef flat (see Figure 2 for location) recorded surface waves as well as water depth and water temperature. Time series plots of this data and a bivarate histogram of the wave period versus the wave height are shown below. The data show that wave height and period are strongly modulated by the tide. Swell waves (periods >6 s) only penetrate over the reef crest during spring high tides.

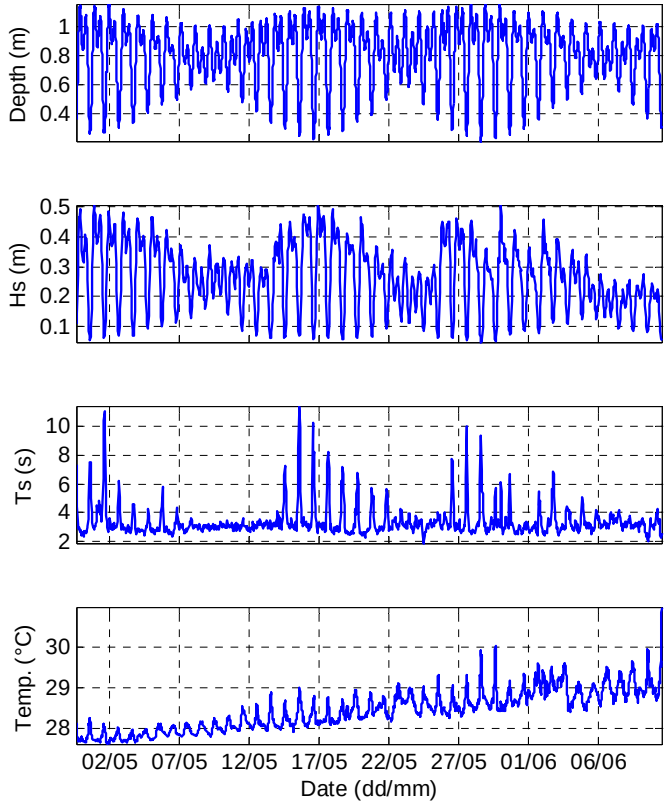

Figure 33. Time series plot of depth (m), significant wave height (Hs), significant wave period (Ts) and temperature (°C) as measured by the TWR on the northern reef flat.

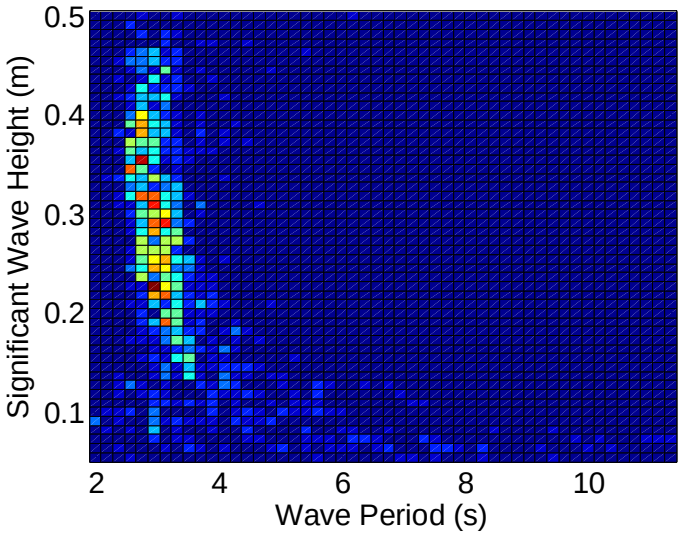

Figure 34. Scatter density plot of significant wave period and wave height for the TWR on the northern reef flat. Blue to red indicates a range from low to high occurrence of a particular bivariate combination.

3.7 TWR Reef Slope South

The TWR on the southern reef slope (see Figure 2 for location) recorded incident surface waves as well as water depth and water temperature. Time series plots of these data and a bivarate histogram of the wave period versus the wave height are shown below. Wave heights were generally 0.2 m with a period of 8 s. Several wind and swell wave events were captured, with the largest height of 1 m recorded during the first week of June.

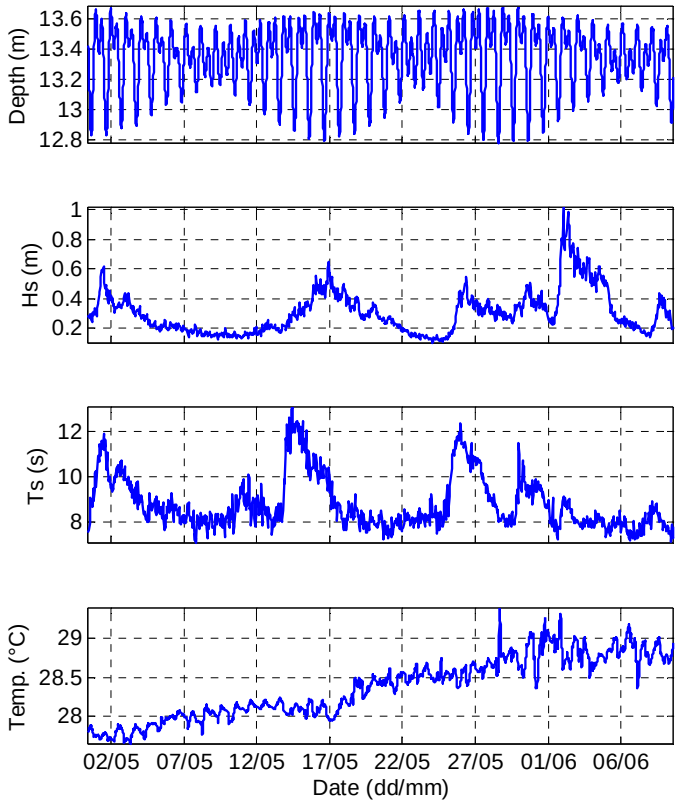

Figure 35. Time series plot of depth (m), significant wave height (Hs), significant wave period (Ts) and temperature (°C) as measured by the TWR on the southern reef slope.

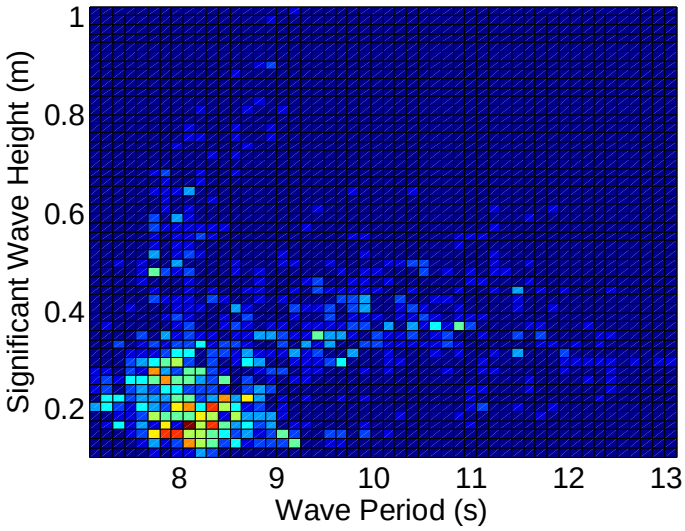

Figure 36. Scatter density plot of significant wave period and wave height for the TWR on the southern reef slope. Blue to red indicates a range from low to high occurrence of a particular bivariate combination.

3.8 TWR Reef Flat South

The TWR on the southern reef flat (see Figure 2 for location) recorded surface waves as well as water depth and water temperature. Time series plots of these data and a bivarate histogram of the wave period versus the wave height are shown below. The data show that wave height, period, and temperature are strongly modulated by the tide. Wave period are distinctly bi-model with periods grouped at either less than 1 s or 5 s. Wave heights are generally low and do not exceed 0.2 m.

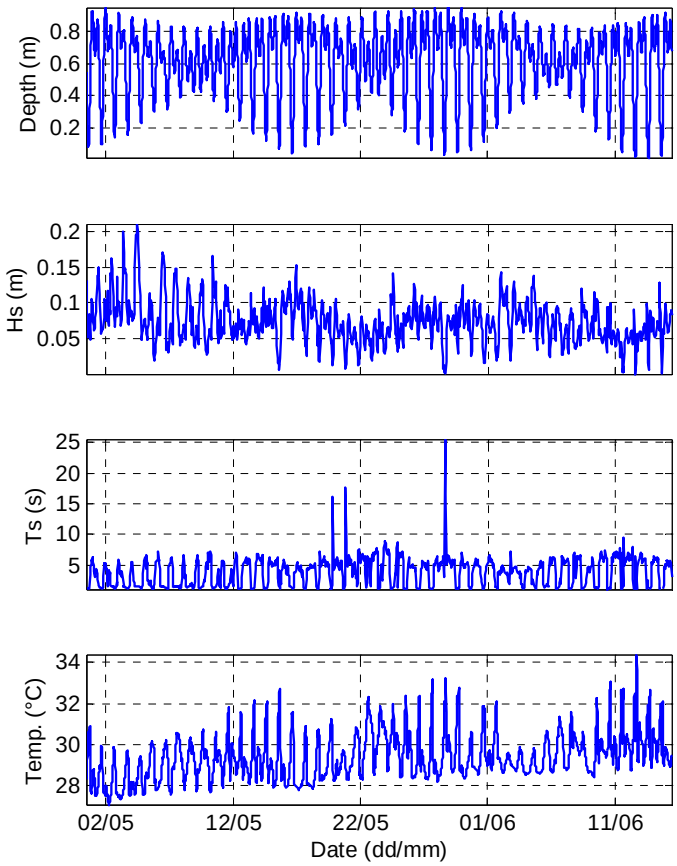

Figure 37. Time series plot of depth (m), significant wave height (Hs), significant wave period (Ts) and temperature (°C) as measured by the TWR on the southern reef flat.

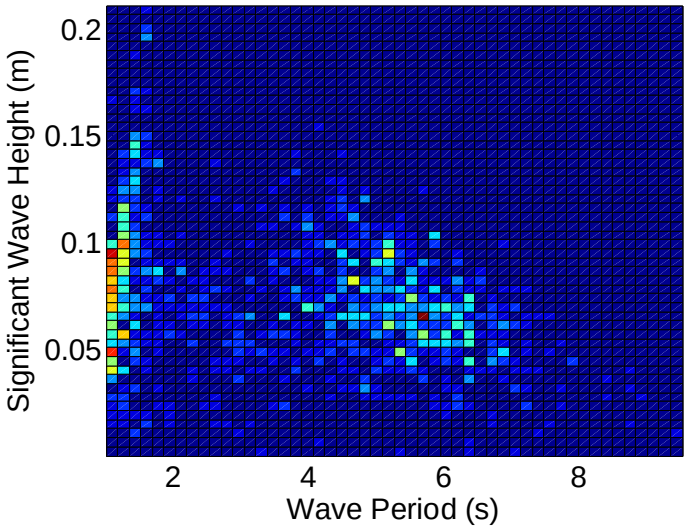

Figure 38. Scatter density plot of significant wave period and wave height for the TWR on the southern reef flat. Blue to red indicates a range from low to high occurrence of a particular bivariate combination.

3.9 Meteorological Data, Saipan Airport Station

The meteorological data obtained from the Saipan airport station are plotted as a time series and wind rose below and show a marked diurnal variability. In general, for the period of observations, the wind can be described as coming from an easterly direction at 4 m/s.

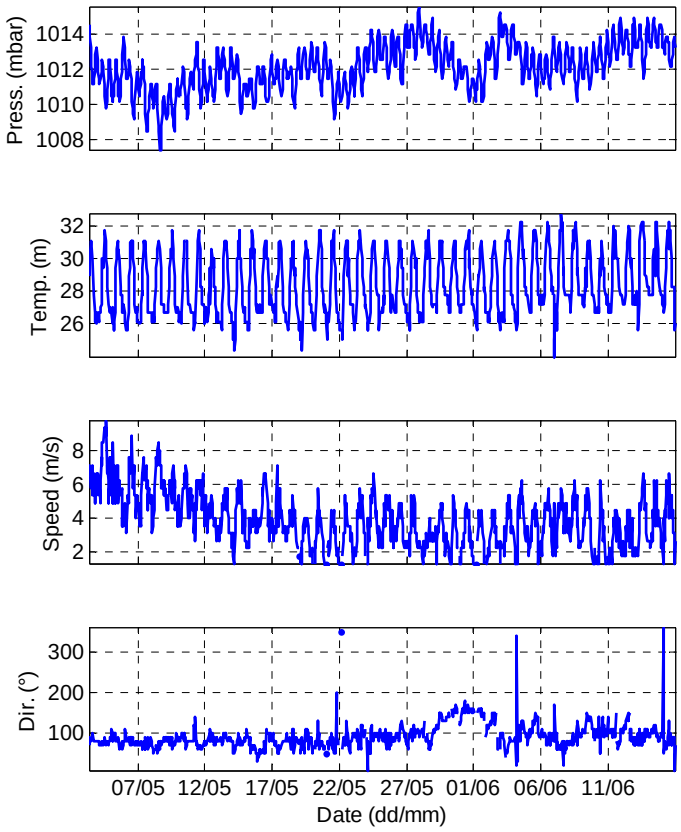

Figure 39. Meteorological parameters collected at the Saipan airport showing time series of air pressure, air temperature, wind speed, and wind direction given in meteorological convention (coming from).

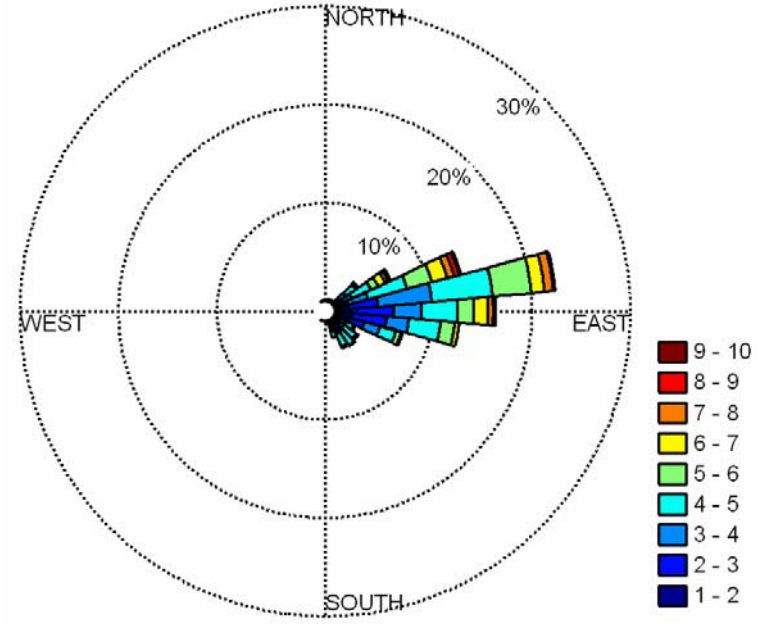

Figure 40. Wind rose for the wind speed and direction shown in Figure 39 above. Direction is given in meteorological convention (coming from). Speed is in m/s.

3.10 ECMWF ERA-Interim Metocean data

Metocean data obtained from the ERA-interim dataset extends from 01/01/1989 to 31/06/2010 at 6-hourly intervals in UTC times. The ERA-interim data was used to compute basic statistical parameters such as minimum, maximum, mean and standard

deviation as shown Table 12 below. Time series plot of wave and wind data over the 20 year period is shown in Figure 41. Density plots and a directional wave rose of significant wave height (Hs), mean wave period (Tm) and mean wave direction (Dm) are shown in Figures 6, 7, 8, 9, 10, and 11, respectively. The data are not reproduced on the Data CD as authorisation for this was not sought from ECMWF.

Table 12. Monthly summary statistics for the ERA-interim wave data

		Jan	Feb	Mar	Apr	May	Jun	Jul	Aug	Sep	Oct	Nov	Dec
Hs	min	1.4	1.3	1.1	1.1	0.9	0.9	0.9	0.8	0.9	1.0	1.2	1.3
	max	4.9	4.7	4.8	4.4	3.1	5.5	4.0	5.0	3.9	7.7	8.4	6.4
	mean	2.5	2.4	2.3	2.0	1.6	1.4	1.4	1.6	1.6	1.9	2.3	2.5
	std	0.5	0.5	0.5	0.4	0.3	0.3	0.4	0.5	0.5	0.5	0.6	0.5
Tm	min	6.8	6.5	6.3	6.1	5.7	5.8	5.5	5.9	5.8	5.8	6.4	6.4
	max	13.0	13.7	13.3	13.3	12.0	10.6	11.6	11.1	12.5	13.2	12.8	13.7
	mean	8.8	8.7	8.6	8.0	7.6	7.2	7.3	7.8	8.0	8.3	8.5	8.8
	std	0.9	1.0	1.0	0.9	0.8	0.7	0.8	0.9	1.1	1.1	1.0	1.0
Dm	min	162.2	155.3	169.2	107.7	12.5	2.7	0.7	0.4	0.2	0.7	13.8	3.0
	max	342.0	275.8	273.8	332.3	357.5	359.4	359.6	360.0	360.0	357.6	355.3	342.1
	mean	226.5	225.8	232.7	247.4	255.0	262.3	258.5	215.1	217.2	228.9	241.4	234.6
	std	21.0	20.3	19.7	19.4	21.6	34.6	64.8	102.8	77.6	49.0	21.6	20.8

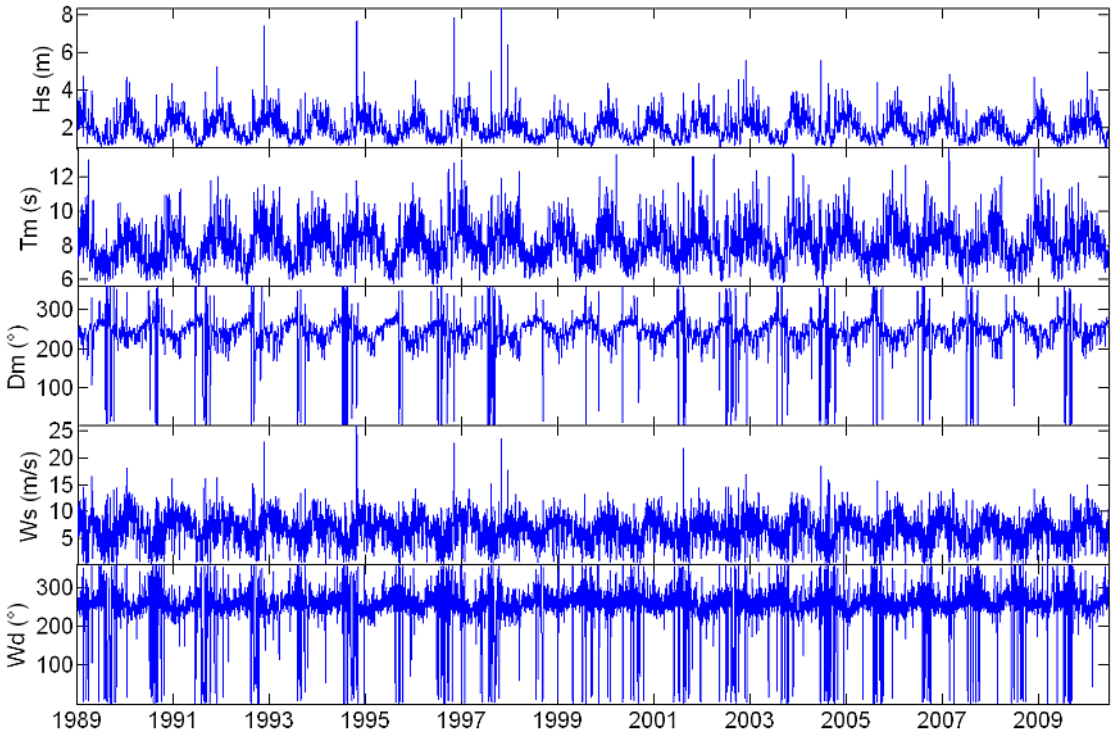

Figure 41. ERA-interim Metocean data time series for the period January 1989 to June 2010. Panels from top to bottom are significant wave height (Hs), mean wave period (Tm), mean wave direction (Dm), wind speed (Ws), and wind direction (Wd). Directions are given in oceanographic convention (going toward).

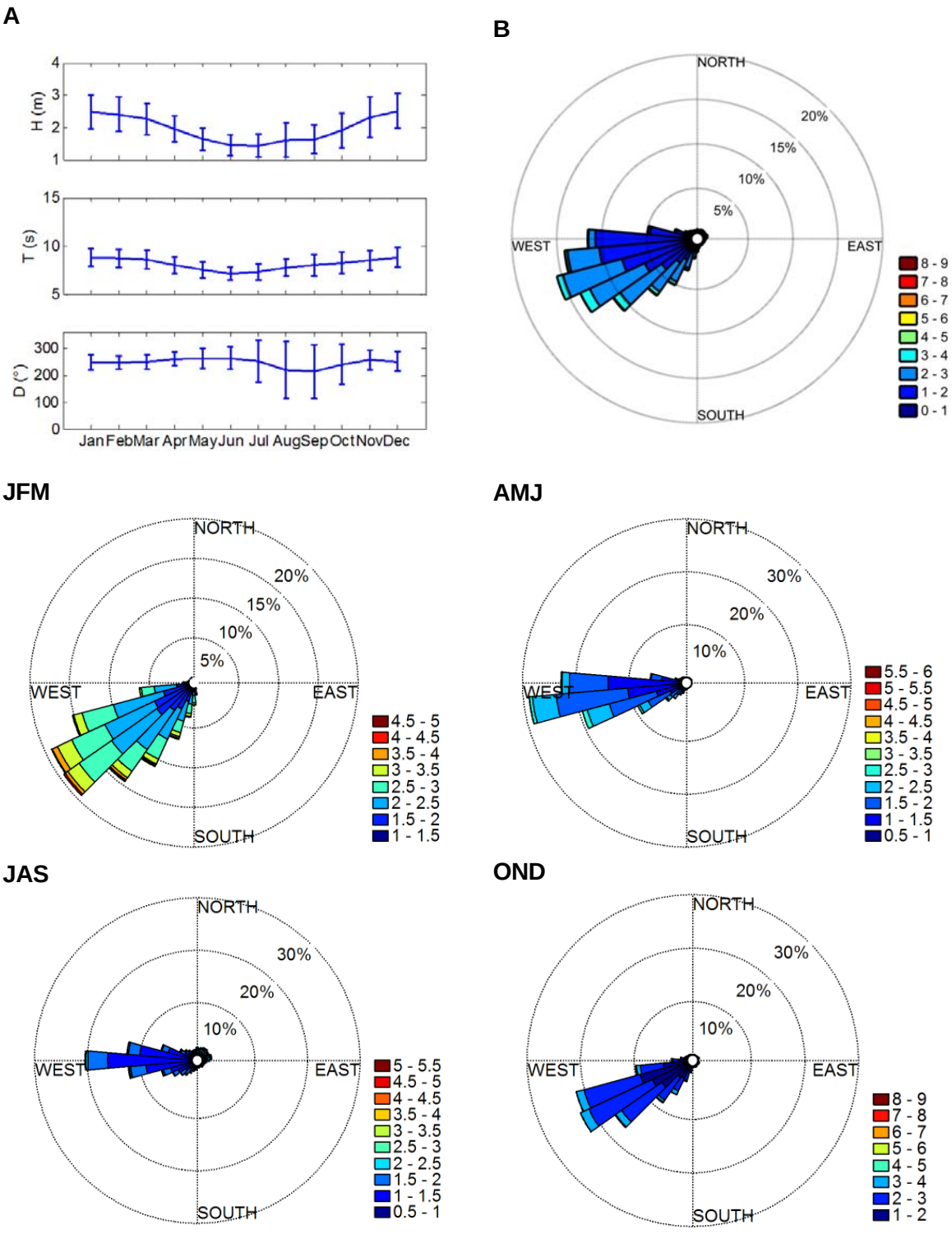

Figure 42. Summary plots of ERA-interim wave data. Panels are from left to right and top to bottom: Panel A shows monthly means and vertical bars of one standard deviation of significant wave height (Hs), mean wave period (Tm), and mean wave direction (Dm); Panel B shows significant wave height in metres and direction as a rose diagram for the entire 20 year dataset; Panel JFM shows a wave rose for the months January, February, and March; Panel AMJ shows the wave rose for April, May and June; Panel JAS shows the wave rose for July, August, and September; and Panel OND shows the wave rose for October, November, and December (OND). Directions are in oceanographic convention (going toward), heights in meters and periods in seconds.

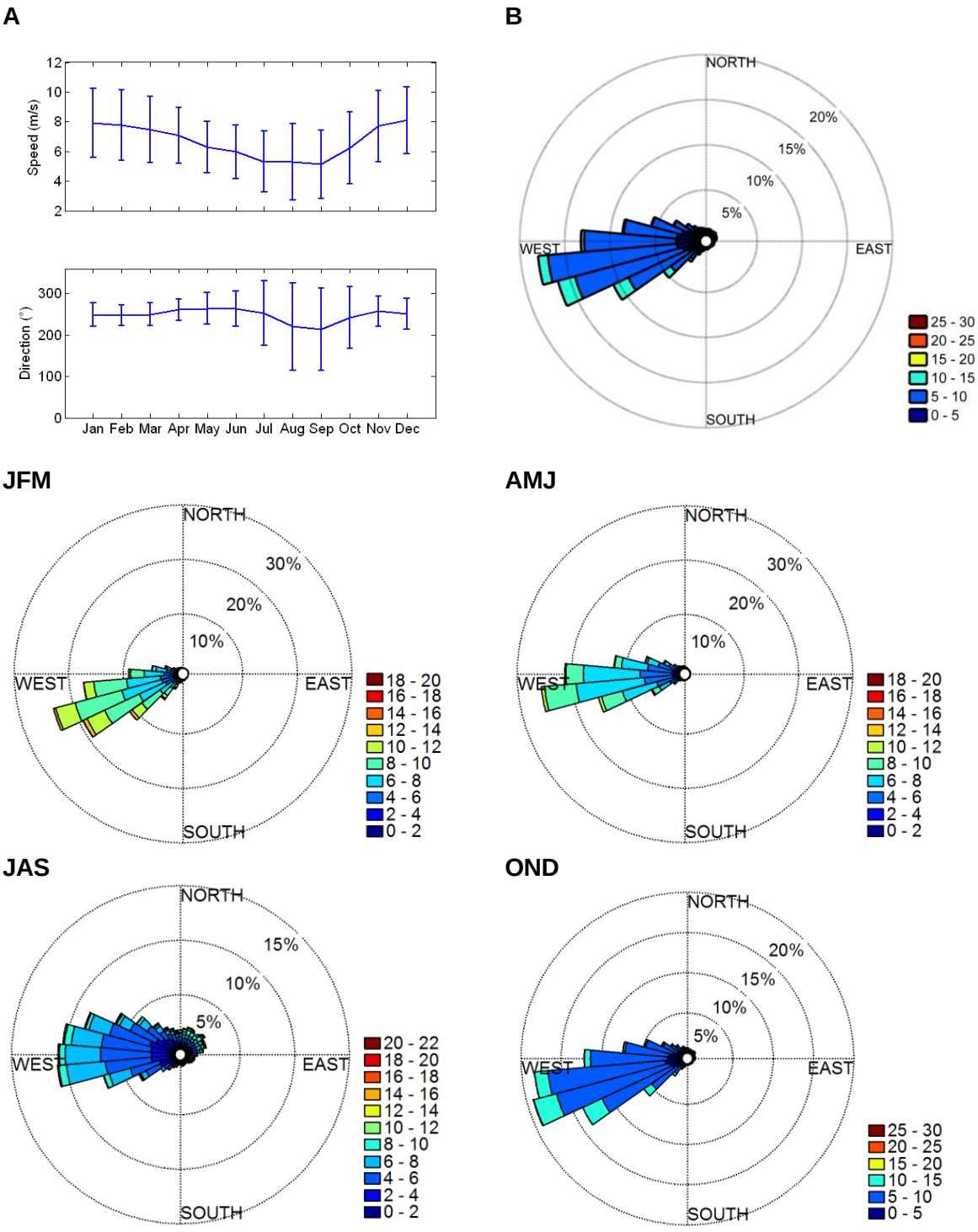

Figure 43. Summary plots of ERA-interim wind data. Panels are from left to right and top to bottom: Panel A shows monthly means and vertical bars of one standard deviation of wind speed and direction; Panel B shows a wind rose for the entire 20 year dataset; Panel JFM shows a wind rose for the months January, February, and March; Panel AMJ shows the wind rose for April, May and June; Panel JAS shows the wind rose for July, August, and September; and Panel OND shows the wind rose for October, November, and December (OND). Directions are in oceanographic convention (going toward) and speeds are in m/s.

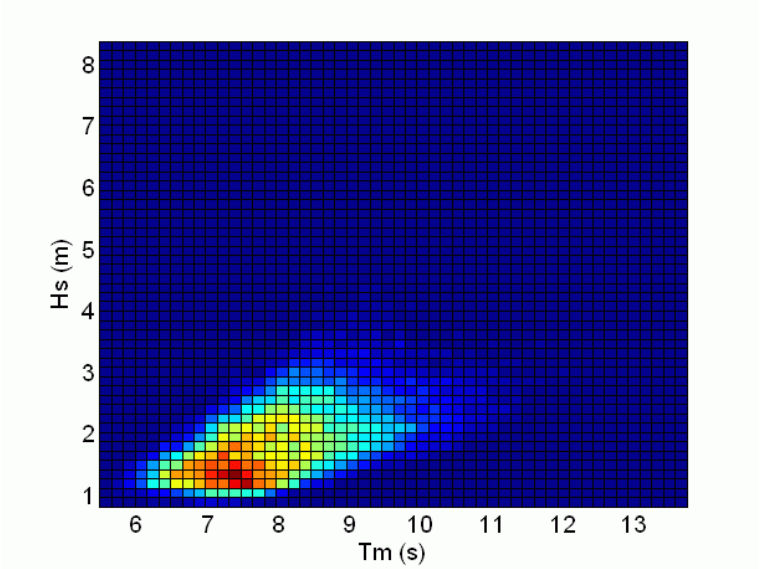

Figure 44: Scatter density plot of mean wave period (Tm), versus significant wave height (Hs) for the ERA-interim dataset. Direction is given from true north in oceanographic convention (going toward). Blue to red indicates a range from low to high occurrence of a particular bivariate combination.

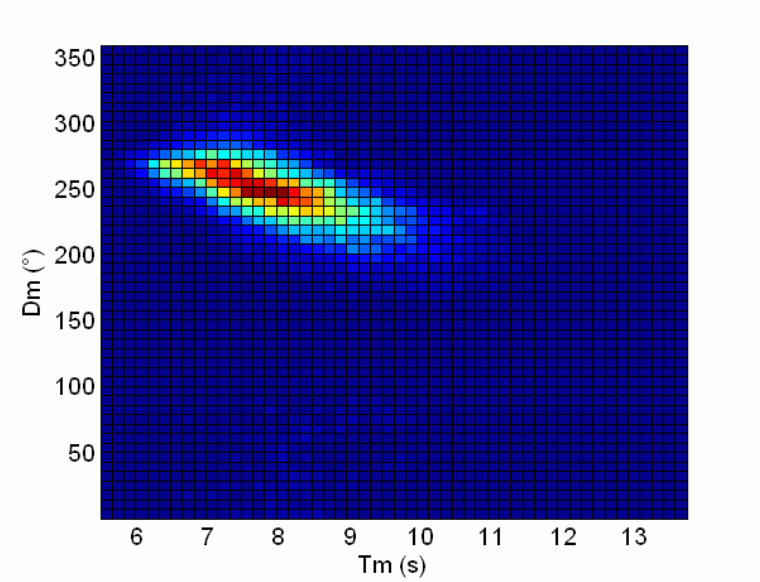

Figure 45: Scatter density plot of mean wave period (Tm) versus mean wave direction (Dm) for the ERA-interim dataset. Direction is given from true north in oceanographic convention (going toward). Blue to red indicates a range from low to high occurrence of a particular bivariate combination.

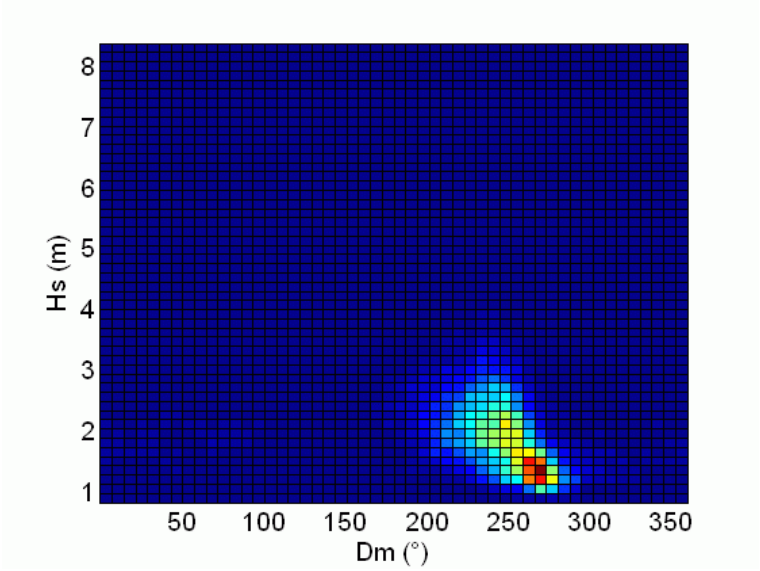

Figure 46: Scatter density plot of mean wave direction (Dm) versus significant wave height (Hs) for the ERA-interim dataset. Direction is given from true north in oceanographic convention (going toward). Blue to red indicates a range from low to high occurrence of a particular bivariate combination.

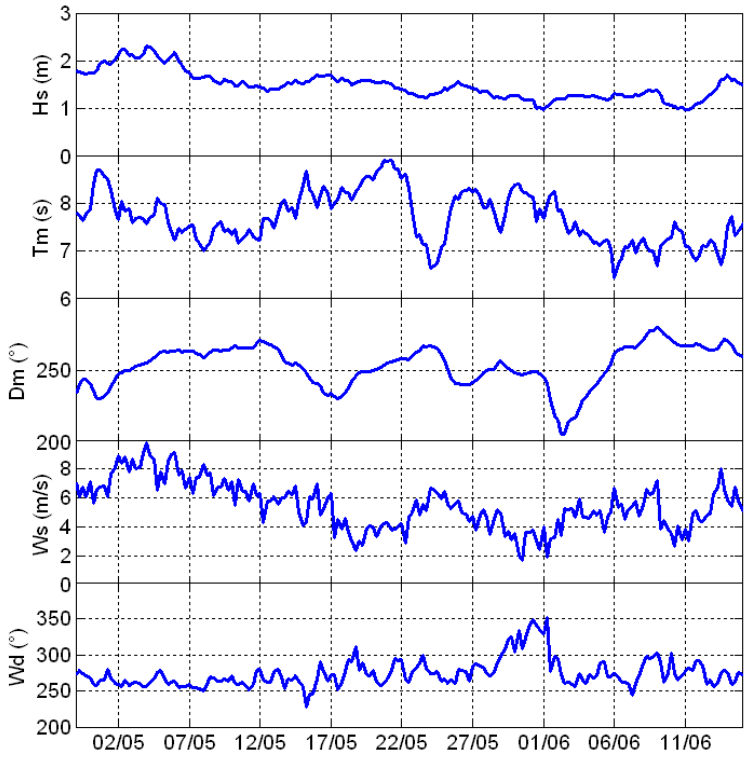

Figure 47. Time series of the ERA-interim metocean data for the period 1/5 to Panels from top to bottom show significant wave height (Hs), mean wave period (Tm), mean wave direction (Dm), wind speed (Ws), and wind direction (Wd).

3.11 GNSS survey data

A total of 1576 GNSS survey points passed the acceptance criteria during baseline processing. 253 points, or 14 %, failed the criteria and were removed from the dataset. The mean height of the points collected along the reef crest was -0.51 m (standard deviation of 0.12, minimum of -1.12 m and maximum of 0.09 m). Figure 48 shows a map of selected surveyed elevations. It was difficult to capture the highest points of the barrier reef due to heavy swells at the time of the survey. The measured heights are therefore assumed to be slightly lower than the true elevation of the barrier reef crest. The literature reports the height of living coral to generally be limited within the envelope of mean low water spring and mean low water neap (e.g. Smithers and Woodroffe, 2000). Hence, it can be assumed that live coral on the barrier reef reach at least a height that is equivalent to the mean lower-low water (MLLW), or 0.39 m below mean sea level defined by the NMVD03. A level of MLLW was therefore assigned to the reef in the domain of the hydrodynamic model (refer to Table 13 for vertical datum definitions). Uplift or subsidence was not considered as Dickinson (2000) concluded that Saipan is in a tectonically stable region.

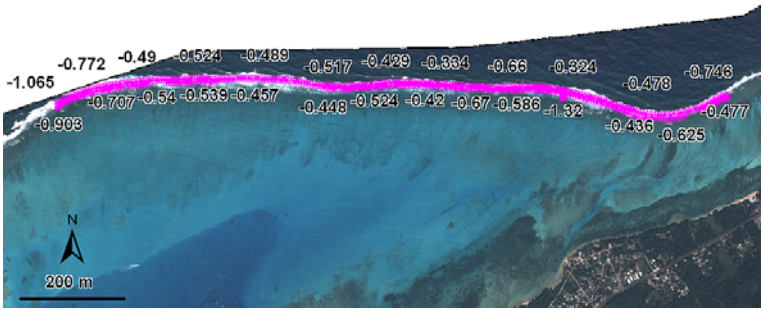

Figure 48. Selected spot heights as surveyed on the barrier reef crest in the northern lagoon. Heights are given relative to NMVD 03. Backdrop is an unrectified 2005 Quickbird image supplied by CRMO.

Table 13. Tide gauge datums relative to mean sea level (source: tidesandcurrents.noaa.gov)		
Datum	Value	Description
MHHW	0.277	Mean Higher-High Water
MHW	0.237	Mean High Water
DTL	-0.057	Mean Diurnal Tide Level
MTL	0.015	Mean Tide Level
MSL	0.000	Mean Sea Level
MLW	-0.207	Mean Low Water
MLLW	-0.392	Mean Lower-Low Water

The results of the shoreline survey at Managaha Island, Puntan Muchot, Sugar Dock, and San Antonio are shown in the figures below. Rectified aerial photographs or satellite imagery was not available at the time of writing, and the image overlays shown below are not indicative of any real on-the-ground variations.

Figure 49. Upper beach (pink line) and the toe of beach (yellow line) for Managaha Island. Backdrop is an unrectified 2005 Quickbird image supplied by CRMO.

Figure 50. Upper beach (pink line) and the toe of beach (yellow line) for Puntan Muchot (Memorial Park). Backdrop is an unrectified 2005 Quickbird image supplied by CRMO.

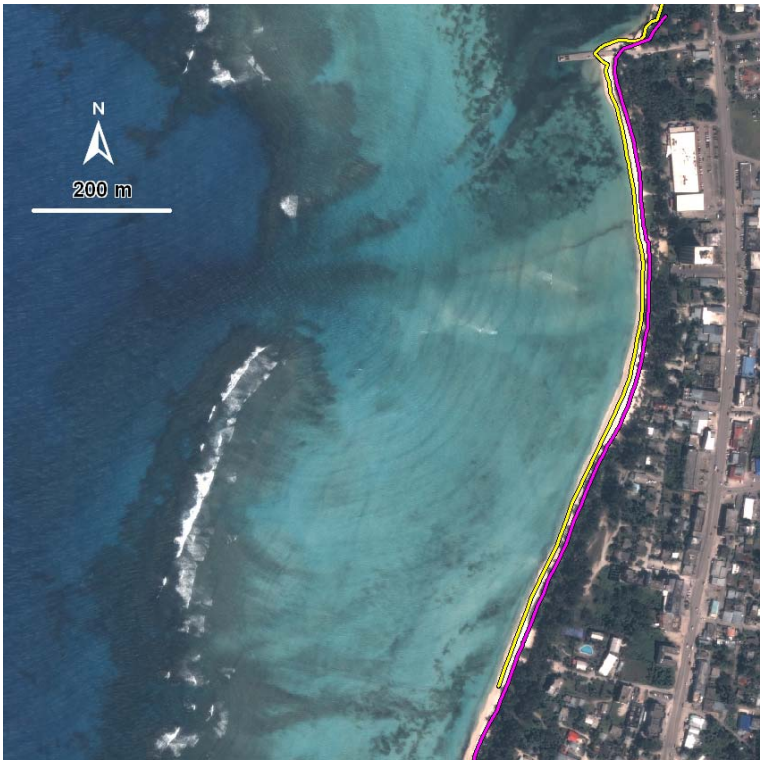

Figure 51. Upper beach (pink line) and the toe of beach (yellow line) for Sugar Dock. Backdrop is an unrectified 2005 Quickbird image supplied by CRMO.

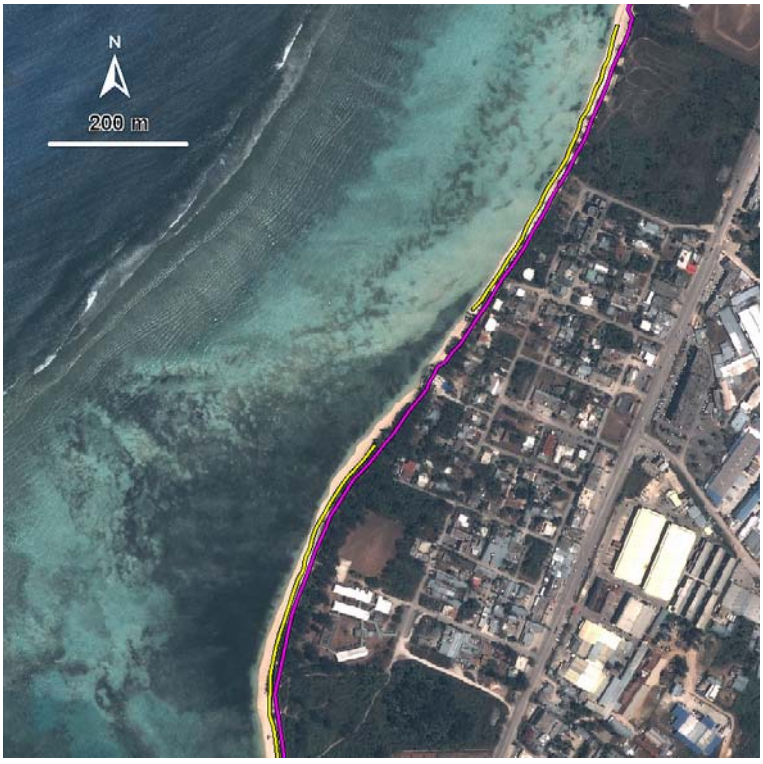

Figure 52. Upper beach (pink line) and the toe of beach (yellow line) for San Antonio. Backdrop is an unrectified 2005 Quickbird image supplied by CRMO.

3.12 Geocoded Photos

A total of 326 geocoded photos were produced providing a detailed record of the state of shoreline along Managaha Island, Puntan Muchot, Sugar Dock, and San Antonio (see Table 14). The photos and accompanying KMZ files for display in Google Earth as shown in Figure 53 are provided on the Data CD. The location of each photo is plotted and labelled by file names in Figure 54 (Managaha Island), Figure 55 (Puntan Muchot

north), Figure 56 (Puntan Muchot south), Figure 57 (Sugar Dock north), Figure 58 (Sugar Dock south), Figure 59 (San Antonio north), Figure 60 (San Antonio south), below.

Table 14. Photo mapping summary		
Date	Location	Photo numbers
6/05/2010	Puntan Muchot	1-83
7/05/2010	Managaha Island	84-141
8/05/2010	Sugar Dock	142-232
8/05/2010	San Antonio	233-274
9/05/2010	Puntan Muchot	275-330

Figure 53. GPS track and geocoded picture thumbnails at Managaha Island displayed from the KMZ file in Google Earth. Clicking on individual or groups of photos causes Google Earth to display larger size pop outs (e.g. the two pictures in the lower right hand corner). Full resolution photos can also be displayed. Geocoded photos were generated with GPicSync (see Methods section for details).

Figure 54. Location of geocoded photos by filename at Managaha Island. Geographic coordinates and photos are provided on the Data CD. Backdrop is an unrectified 2003 IKONOS satellite image provided by CRMO.

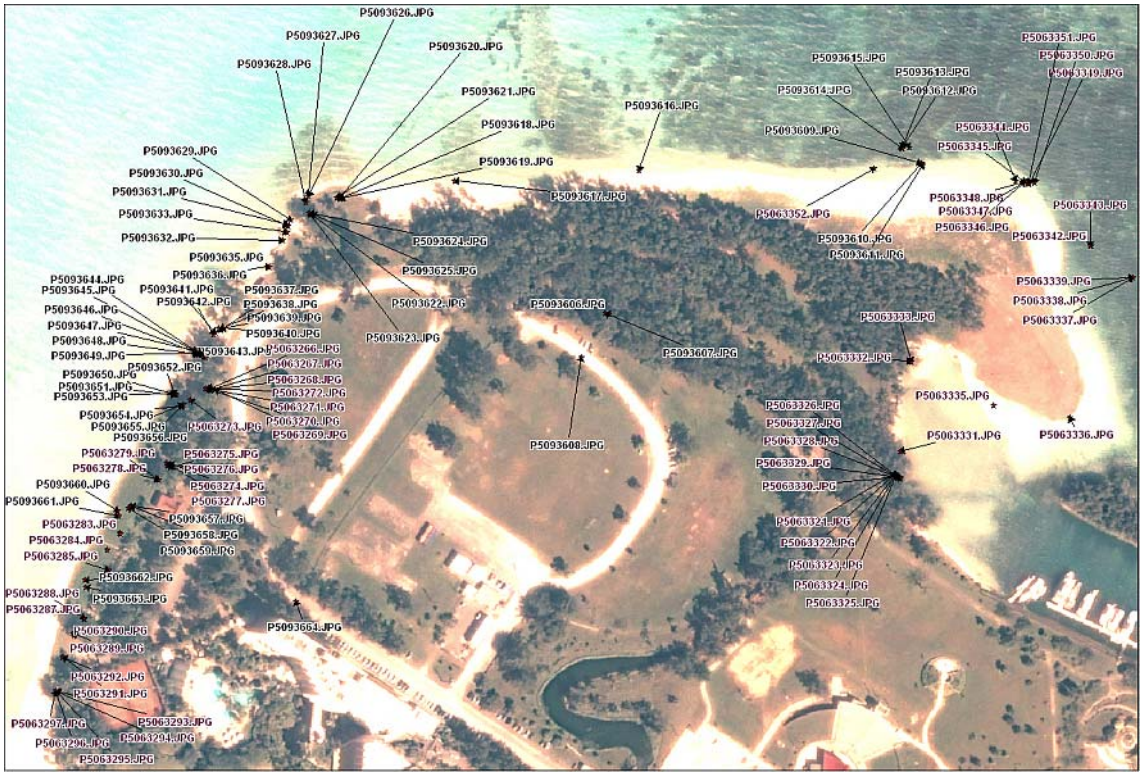

Figure 55. Location of geocoded photos by filename at Puntan Muchot north (Memorial Park). Geographic coordinates and photos are provided on the Data CD. Backdrop is an unrectified 2003 IKONOS satellite image provided by CRMO.

Figure 56. Location of geocoded photos by filename at Puntan Muchot south. Geographic coordinates and photos are provided on the Data CD. Backdrop is an unrectified 2003 IKONOS satellite image provided by CRMO.

Figure 57. Location of geocoded photos by filename at Sugar Dock north. Geographic coordinates and photos are provided on the Data CD. Backdrop is an unrectified 2003 IKONOS satellite image provided by CRMO.

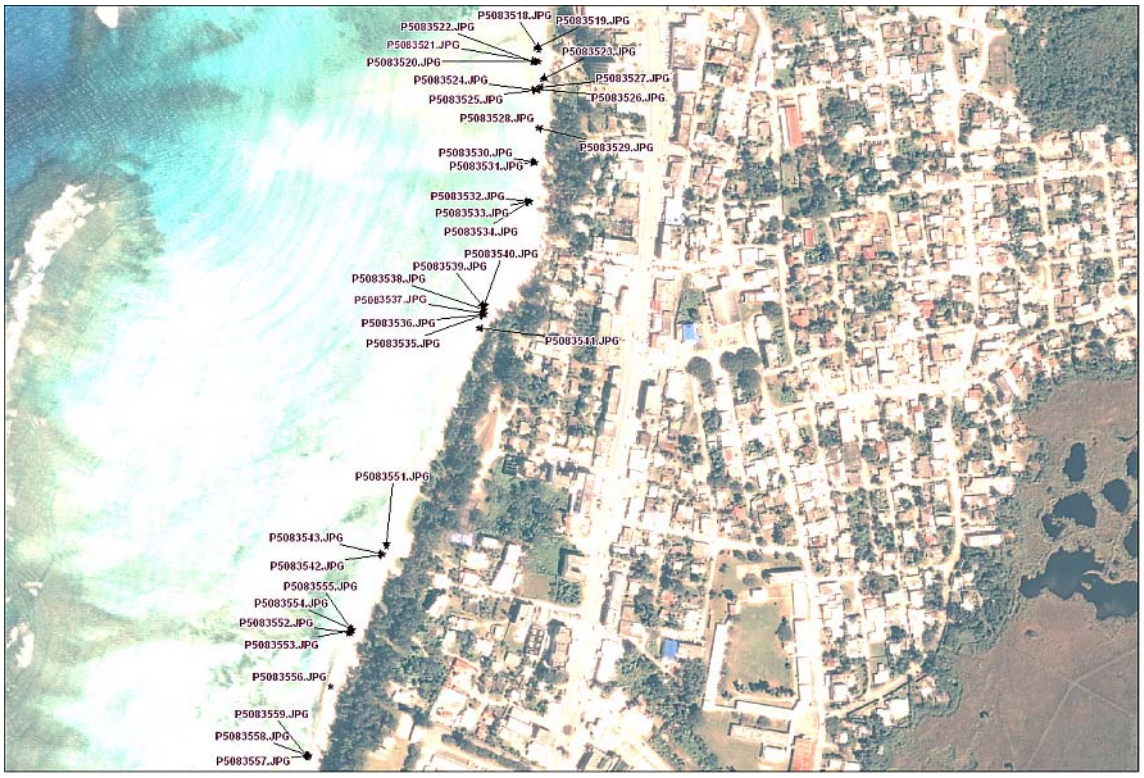

Figure 58. Location of geocoded photos by filename south of Sugar Dock. Geographic coordinates and photos are provided on the Data CD. Backdrop is an unrectified 2003 IKONOS satellite image provided by CRMO.

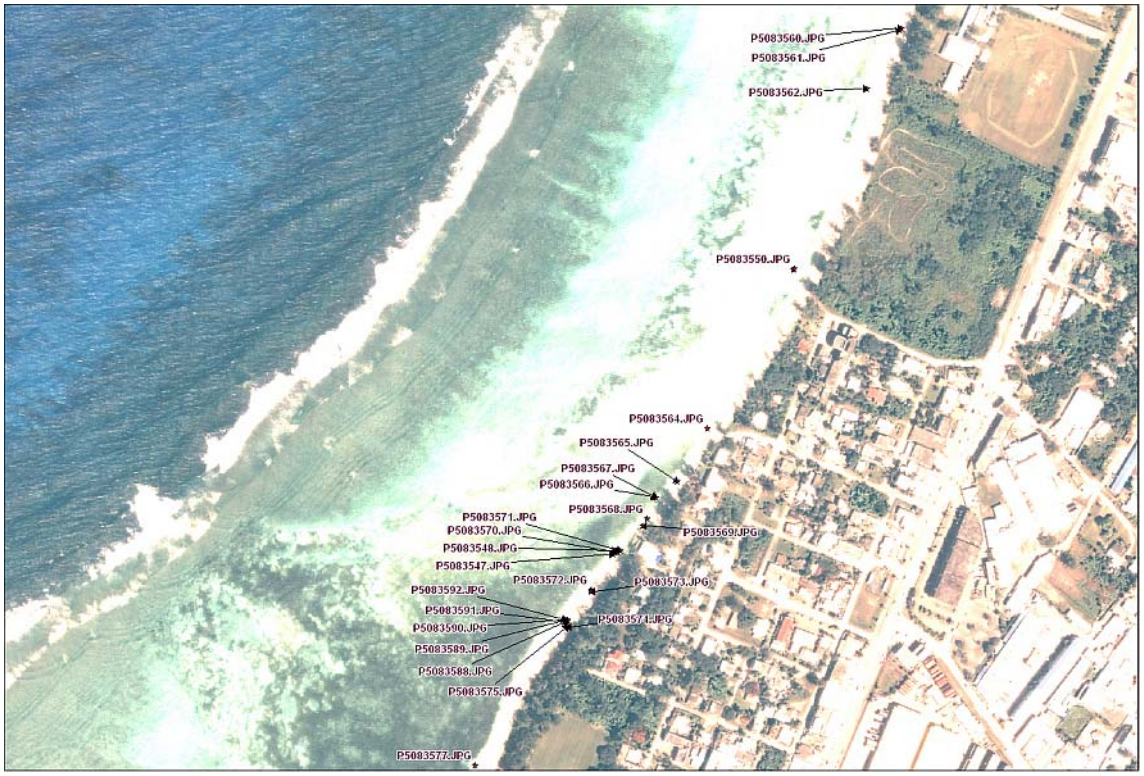

Figure 59. Location of geocoded photos by filename north at San Antonio. Geographic coordinates and photos are provided on the Data CD. Backdrop is an unrectified 2003 IKONOS satellite image provided by CRMO.

Figure 60. Location of geocoded photos by filename south of San Antonio. Geographic coordinates and photos are provided on the Data CD. Backdrop is an unrectified 2003 IKONOS satellite image provided by CRMO.

3.13 Sediment samples

All sediment samples comprised of poorly sorted very fine gravely coarse sand with an average mean grain size of 0.8 mm. Detailed results of the grain size distribution analysis are given in the Data CD and summary statistics are presented in the figures below.

SAMPLE STATISTICS

SAMPLE IDENTITY: **San Antonio** ANALYST & DATE: SOPAC, 5/5/2010

SAMPLE TYPE: Polymodal, Poorly Sorted TEXTURAL GROUP: Gravelly Sand

SEDIMENT NAME: Very Fine Gravelly Coarse Sand

	µm	ϕ
MODE 1:	605.0	0.747
MODE 2:	1200.0	-0.243
MODE 3:	2400.0	-1.243
D_{10}:	262.6	-1.101
MEDIAN or D_{50}:	676.0	0.565
D_{90}:	2145.6	1.929
(D_{90} / D_{10}):	8.170	-1.751
(D_{90} - D_{10}):	1883.0	3.030
(D_{75} / D_{25}):	2.329	-3.066
(D_{75} - D_{25}):	702.6	1.220

GRAIN SIZE DISTRIBUTION

GRAVEL: 12.6%	COARSE SAND: 35.6%
SAND: 87.4%	MEDIUM SAND: 10.9%
MUD: 0.0%	FINE SAND: 8.5%
	V FINE SAND: 0.0%
V COARSE GRAVEL: 0.0%	V COARSE SILT: 0.0%
COARSE GRAVEL: 0.0%	COARSE SILT: 0.0%
MEDIUM GRAVEL: 0.0%	MEDIUM SILT: 0.0%
FINE GRAVEL: 0.0%	FINE SILT: 0.0%
V FINE GRAVEL: 12.6%	V FINE SILT: 0.0%
V COARSE SAND: 32.4%	CLAY: 0.0%

	METHOD OF MOMENTS			FOLK & WARD METHOD		
	Arithmetic µm	Geometric µm	Logarithmic ϕ	Geometric µm	Logarithmic ϕ	Description
MEAN ($\bar{x}$):	953.2	730.7	0.453	662.8	0.593	Coarse Sand
SORTING (σ):	654.1	2.120	1.084	2.181	1.125	Poorly Sorted
SKEWNESS (Sk):	1.069	-0.416	0.416	-0.054	0.054	Symmetrical
KURTOSIS (K):	3.357	2.705	2.705	1.338	1.338	Leptokurtic

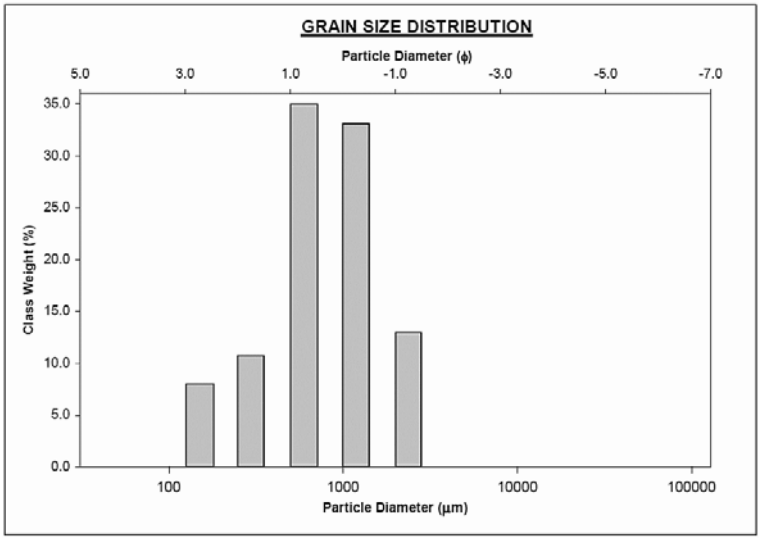

Figure 61. Sample statistics and grain size distribution for the beach sediment sample taken at San Antonio.

SAMPLE STATISTICS

SAMPLE IDENTITY: **Sugar Dock** ANALYST & DATE: SOPAC, 5/8/2010

SAMPLE TYPE: Polymodal, Poorly Sorted TEXTURAL GROUP: Gravelly Sand

SEDIMENT NAME: Very Fine Gravelly Coarse Sand

	μm	ϕ
MODE 1:	605.0	0.747
MODE 2:	302.5	1.747
MODE 3:	1200.0	-0.243
D_{10}:	254.8	-0.442
MEDIAN or D_{50}:	560.8	0.834
D_{90}:	1358.4	1.973
(D_{90} / D_{10}):	5.331	-4.463
(D_{90} - D_{10}):	1103.6	2.415
(D_{75} / D_{25}):	2.306	3.385
(D_{75} - D_{25}):	399.0	1.205

GRAIN SIZE DISTRIBUTION

GRAVEL: 8.6%	COARSE SAND: 38.4%
SAND: 91.4%	MEDIUM SAND: 29.0%
MUD: 0.0%	FINE SAND: 8.4%
	V FINE SAND: 0.0%
V COARSE GRAVEL: 0.0%	V COARSE SILT: 0.0%
COARSE GRAVEL: 0.0%	COARSE SILT: 0.0%
MEDIUM GRAVEL: 0.0%	MEDIUM SILT: 0.0%
FINE GRAVEL: 0.0%	FINE SILT: 0.0%
V FINE GRAVEL: 8.6%	V FINE SILT: 0.0%
V COARSE SAND: 15.5%	CLAY: 0.0%

	METHOD OF MOMENTS			FOLK & WARD METHOD		
	Arithmetic	Geometric	Logarithmic	Geometric	Logarithmic	Description
	μm	μm	ϕ	μm	ϕ	
MEAN ($\bar{x}$):	726.1	543.5	0.880	568.0	0.816	Coarse Sand
SORTING (σ):	601.2	2.088	1.048	2.174	1.120	Poorly Sorted
SKEWNESS (Sk):	1.756	0.273	-0.273	0.037	-0.037	Symmetrical
KURTOSIS (K):	5.374	2.616	2.616	1.323	1.323	Leptokurtic

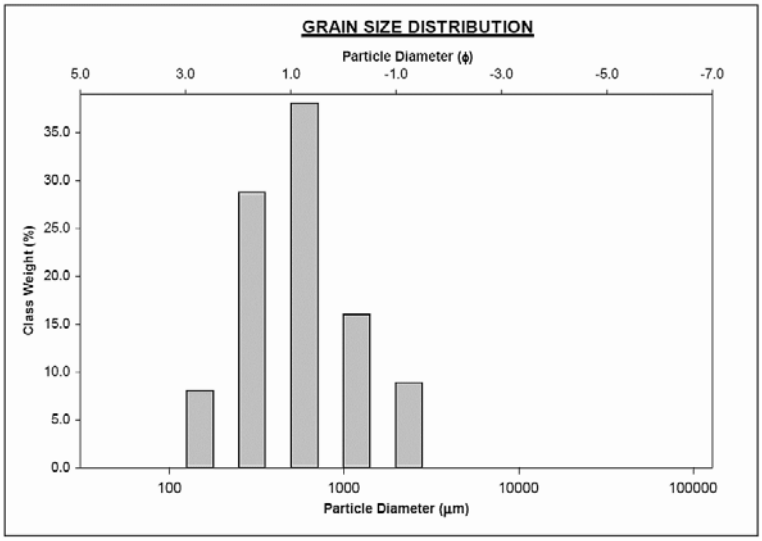

Figure 62. Sample statistics and grain size distribution for the beach sediment sample taken at Sugar Dock.

SAMPLE STATISTICS

SAMPLE IDENTITY: **Managaha Is.** ANALYST & DATE: SOPAC, 5/7/2010

SAMPLE TYPE: Trimodal, Poorly Sorted TEXTURAL GROUP: Gravelly Sand

SEDIMENT NAME: Very Fine Gravelly Coarse Sand

	µm	ϕ
MODE 1:	605.0	0.747
MODE 2:	302.5	1.747
MODE 3:	1200.0	-0.243
D_{10}:	268.1	-0.364
MEDIAN or D_{50}:	587.6	0.767
D_{90}:	1287.0	1.899
(D_{90} / D_{10}):	4.801	-5.218
(D_{90} - D_{10}):	1019.0	2.263
(D_{75} / D_{25}):	1.353	1.795
(D_{75} - D_{25}):	178.4	0.436

GRAIN SIZE DISTRIBUTION

GRAVEL: 7.1%	COARSE SAND: 58.0%
SAND: 92.9%	MEDIUM SAND: 16.6%
MUD: 0.0%	FINE SAND: 6.7%
	V FINE SAND: 0.0%
V COARSE GRAVEL: 0.0%	V COARSE SILT: 0.0%
COARSE GRAVEL: 0.0%	COARSE SILT: 0.0%
MEDIUM GRAVEL: 0.0%	MEDIUM SILT: 0.0%
FINE GRAVEL: 0.0%	FINE SILT: 0.0%
V FINE GRAVEL: 7.1%	V FINE SILT: 0.0%
V COARSE SAND: 11.6%	CLAY: 0.0%

	METHOD OF MOMENTS			FOLK & WARD METHOD		
	Arithmetic	Geometric	Logarithmic	Geometric	Logarithmic	Description
	µm	µm	ϕ	µm	ϕ	
MEAN ($\bar{x}$):	720.9	578.2	0.790	578.3	0.790	Coarse Sand
SORTING (σ):	534.0	1.876	0.908	2.036	1.026	Poorly Sorted
SKEWNESS (Sk):	2.122	0.113	-0.113	-0.010	0.010	Symmetrical
KURTOSIS (K):	7.158	3.599	3.599	3.523	3.523	Extremely Leptokurtic

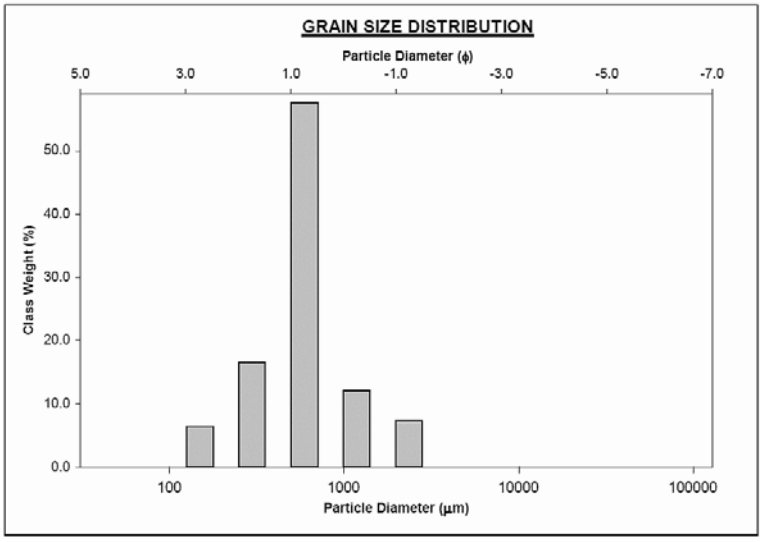

Figure 63. Sample statistics and grain size distribution for the beach sediment sample taken at Managaha Island.

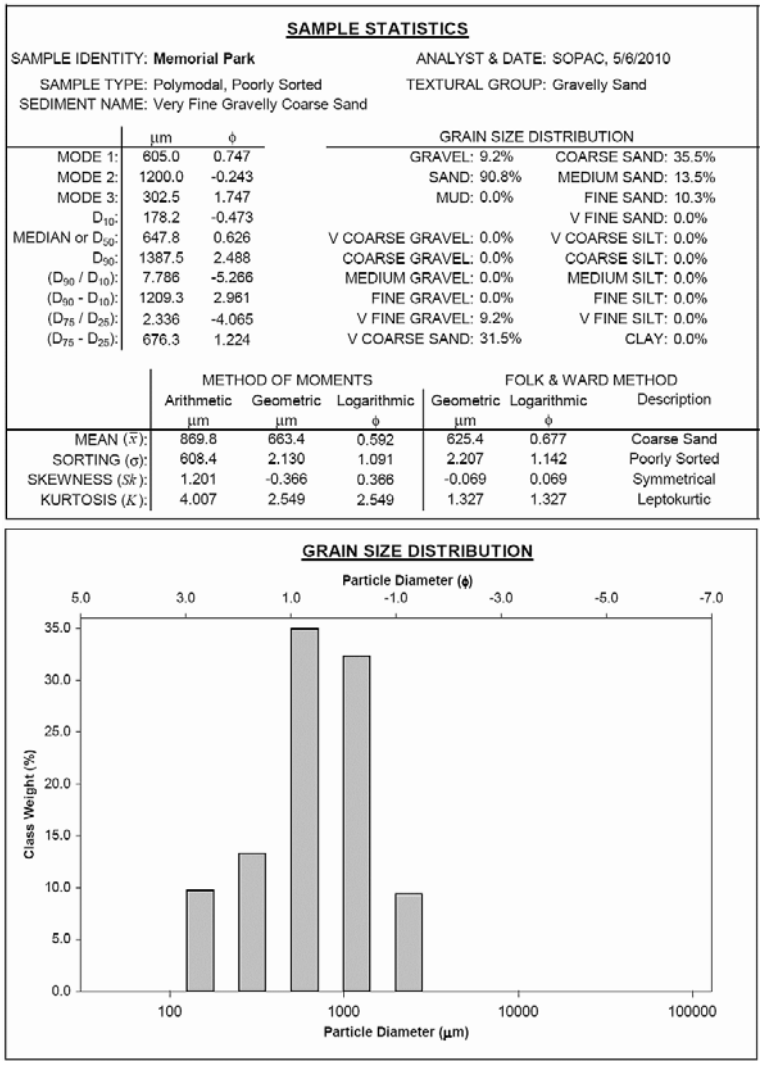

SAMPLE STATISTICS

SAMPLE IDENTITY: **Memorial Park** ANALYST & DATE: SOPAC, 5/6/2010

SAMPLE TYPE: Polymodal, Poorly Sorted TEXTURAL GROUP: Gravelly Sand

SEDIMENT NAME: Very Fine Gravelly Coarse Sand

	µm	ϕ
MODE 1:	605.0	0.747
MODE 2:	1200.0	-0.243
MODE 3:	302.5	1.747
D_{10}:	178.2	-0.473
MEDIAN or D_{50}:	647.8	0.626
D_{90}:	1387.5	2.488
(D_{90} / D_{10}):	7.786	-5.266
(D_{90} - D_{10}):	1209.3	2.961
(D_{75} / D_{25}):	2.336	-4.065
(D_{75} - D_{25}):	676.3	1.224

GRAIN SIZE DISTRIBUTION

GRAVEL: 9.2%	COARSE SAND: 35.5%
SAND: 90.8%	MEDIUM SAND: 13.5%
MUD: 0.0%	FINE SAND: 10.3%
	V FINE SAND: 0.0%
V COARSE GRAVEL: 0.0%	V COARSE SILT: 0.0%
COARSE GRAVEL: 0.0%	COARSE SILT: 0.0%
MEDIUM GRAVEL: 0.0%	MEDIUM SILT: 0.0%
FINE GRAVEL: 0.0%	FINE SILT: 0.0%
V FINE GRAVEL: 9.2%	V FINE SILT: 0.0%
V COARSE SAND: 31.5%	CLAY: 0.0%

	METHOD OF MOMENTS			FOLK & WARD METHOD		
	Arithmetic µm	Geometric µm	Logarithmic ϕ	Geometric µm	Logarithmic ϕ	Description
MEAN ($\bar{x}$):	869.8	663.4	0.592	625.4	0.677	Coarse Sand
SORTING (σ):	608.4	2.130	1.091	2.207	1.142	Poorly Sorted
SKEWNESS (Sk):	1.201	-0.366	0.366	-0.069	0.069	Symmetrical
KURTOSIS (K):	4.007	2.549	2.549	1.327	1.327	Leptokurtic

Figure 64. Sample statistics and grain size distribution for the beach sediment sample taken at Memorial Park.

The relative abundance of coral fragments, foraminifera, *Halimeda*, and shell pieces, differed significantly between the north and south of the lagoon. The samples taken from the northern part of the lagoon, namely Managaha Island and Puntan Muchot (Memorial Park), show a high abundance (approximately 75%) of coral fragments, whereas the samples taken at Sugar Dock and San Antonio in the south of the lagoon comprise one third each of foraminifera and coral fragments. Shell fragments and *Halimeda* were minor component in all samples varying between 4 to 17% as shown in the table and figure below.

Table 15. Sand Composition Analysis (percentage abundance)

	Coral Fragments	Foraminifera	Shell Fragments	*Halimeda*
San Antonio	38 %	37 %	17 %	8 %
Sugar Dock	41 %	32 %	15 %	12 %
Managaha Is.	78 %	4 %	12 %	6 %
Memorial Park	74 %	8 %	14 %	4 %

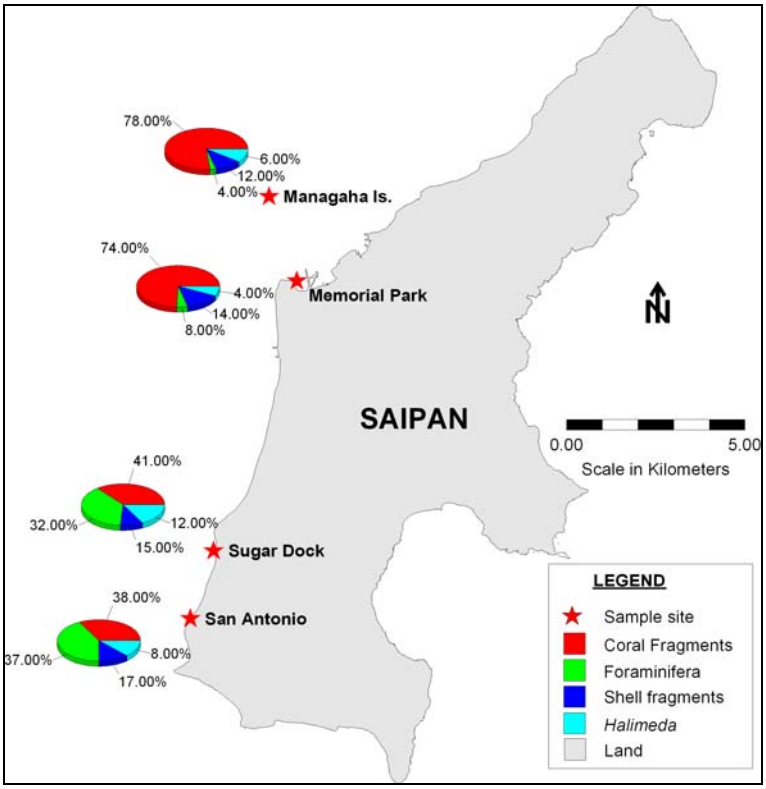

Figure 65. Percentage abundance of major components of the beach sediment samples.

3.14 Wave-Current Hydrodynamic Model

This section presents some calibration results and preliminary snapshots of the hydrodynamic model that was still under preparation at the time of writing. Full model results and runs will be given in a subsequent report. The field data results presented above show a strong coupling between incident wave forcing and lagoon circulation. This prominent feature of the time series data was well reproduced by the three-dimensional coupled wave-current numerical model (see Figure 66 and Figure 67). The model will now be used to derive the distribution patterns of particles discharged from a sewage outfall. It will also be utilised to determine the dominant sediment transport directions under various different seasonal forcing mechanisms.

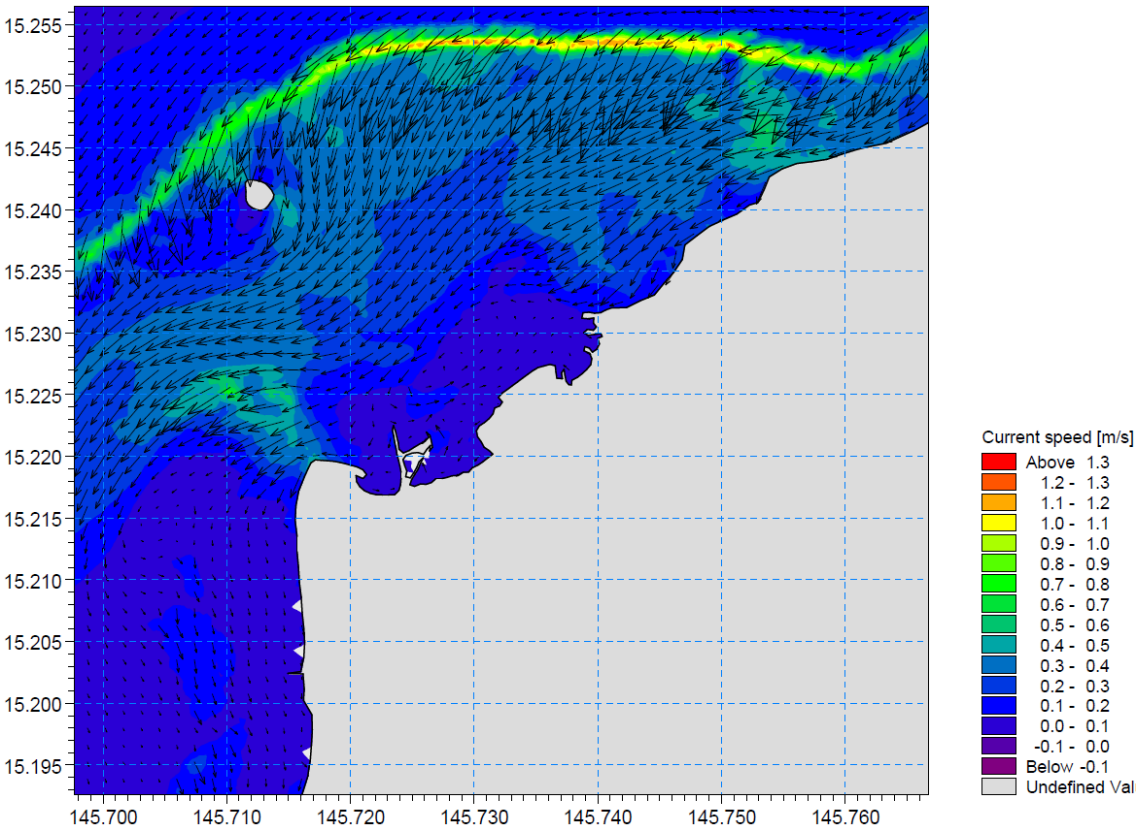

Figure 66. Snapshot of the model showing the current speed and direction (depicted by colour banding and size and direction of vectors) of the surface layer in the northern lagoon at spring high tide. Note that water enters the lagoon over the reef crest, with current speeds exceeding 50 cm/s in the lagoon and a general flow to the southwest.

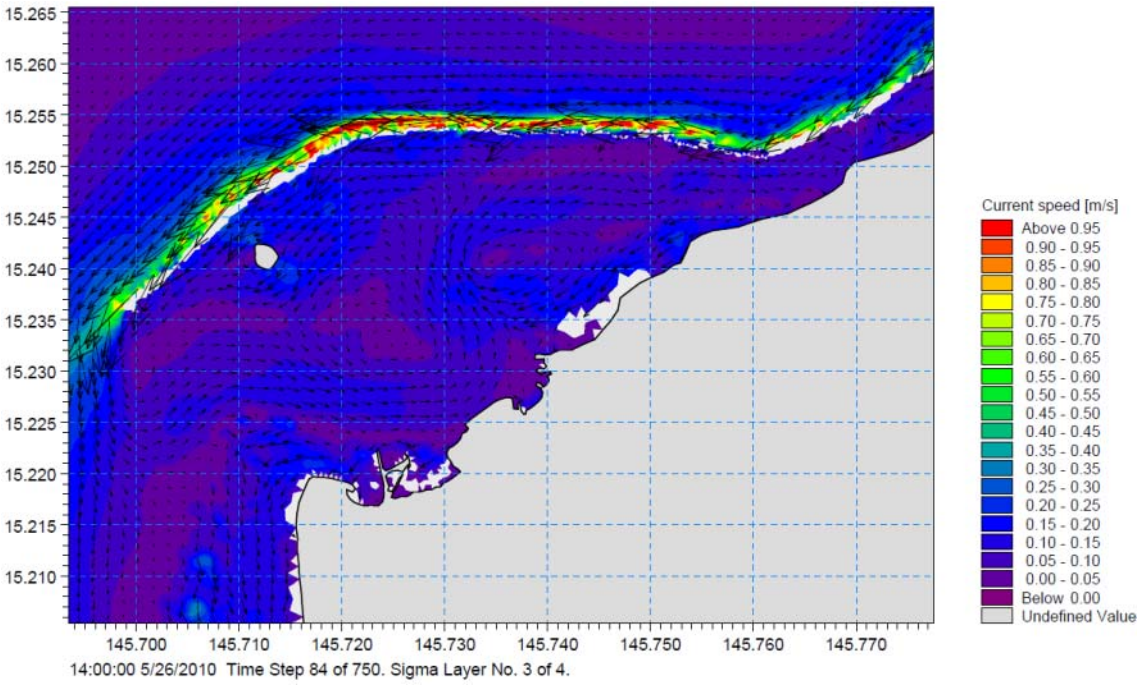

Figure 67. Snapshot of the model showing the current speed and direction (depicted by colour banding and size and direction of vectors) of the surface water layer in the northern lagoon at spring low tide. Note that the barrier reef is shown as partially dry (grey colour) and that current speeds are low (<20 cm/s), with indications of the presence of gyres within the lagoon.

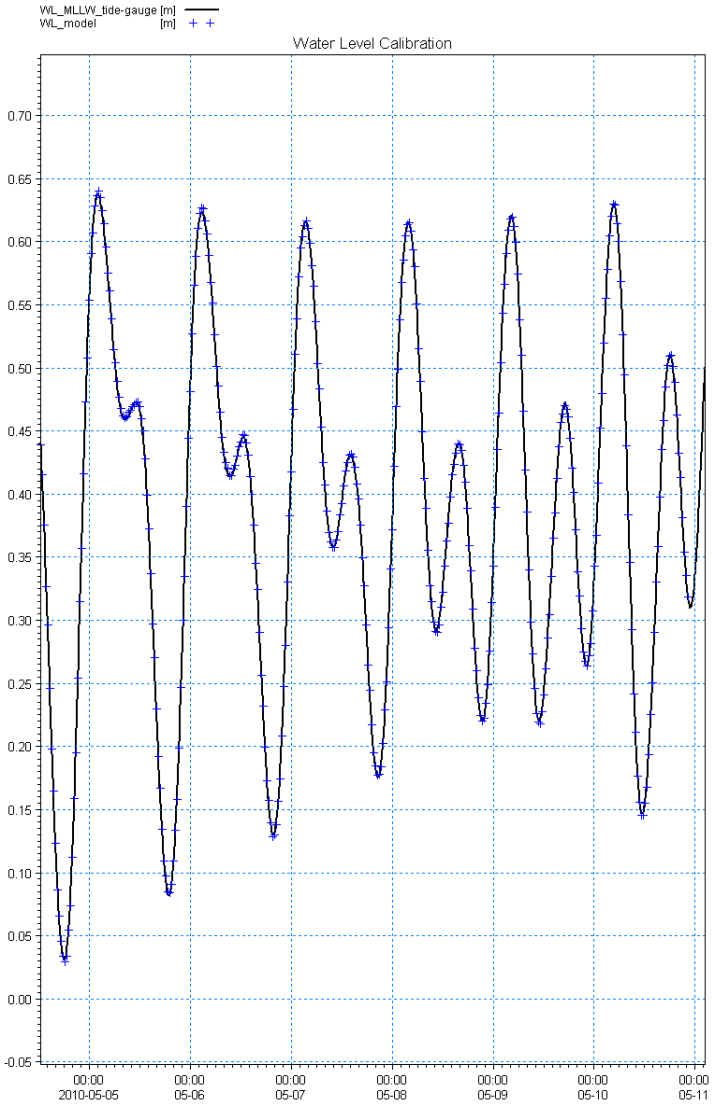

Figure 68. Calibration results showing good agreement between water levels as derived from the model (markers) and those observed by the tide gauge (continuous line). The mean range for Saipan is 0.45 m (the difference in height between mean high water and mean low water). The diurnal range (the difference in height between mean higher high water and mean lower low water) is 0.67 m.

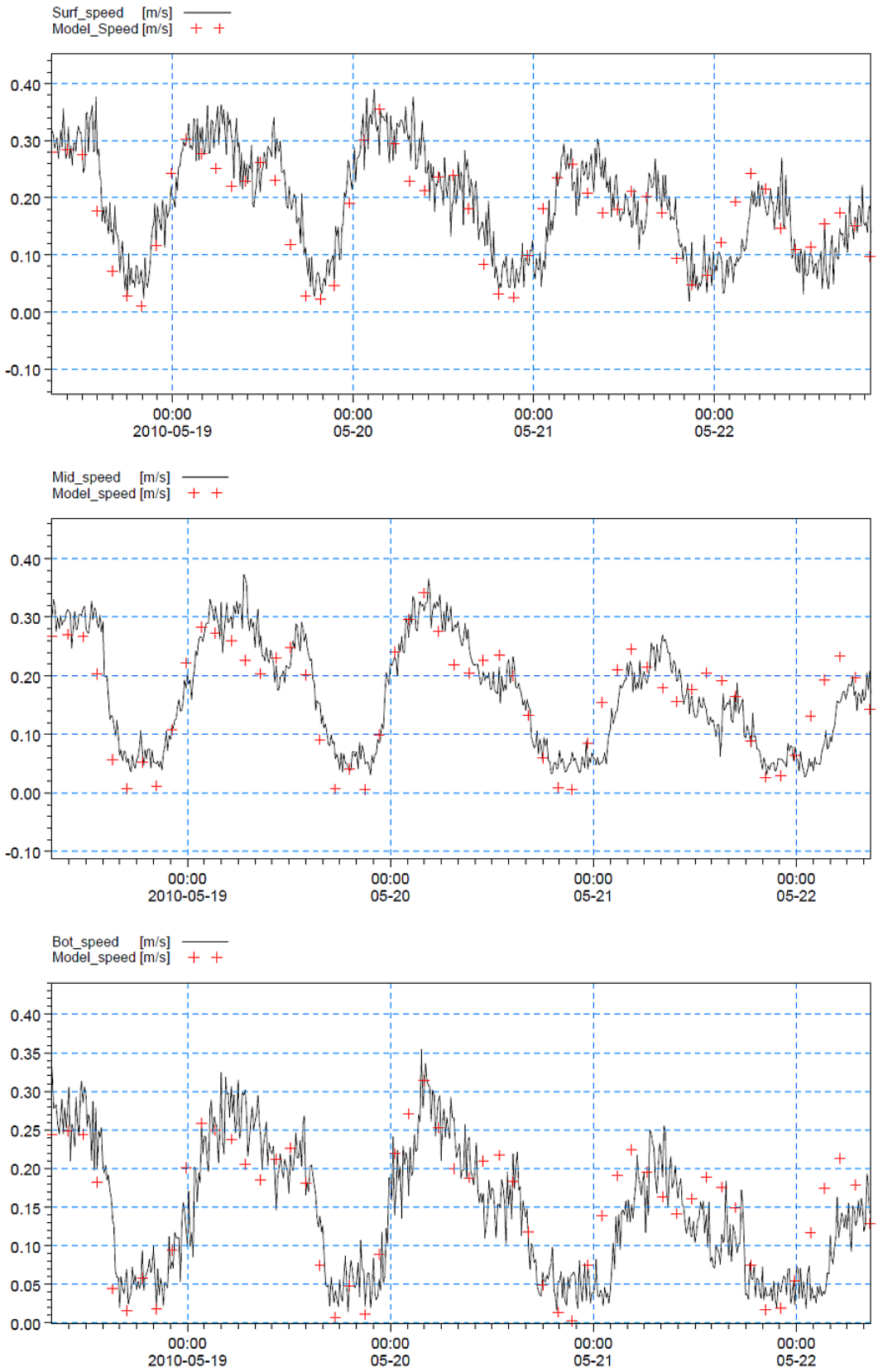

Figure 69. Calibration results showing good agreement between the observed current speed (line) of the surface layer (top panel), mid water layer (centre panel), and near-bed layer (bottom panel), and those obtained from the model (crosses) for the ADP location in the channel.

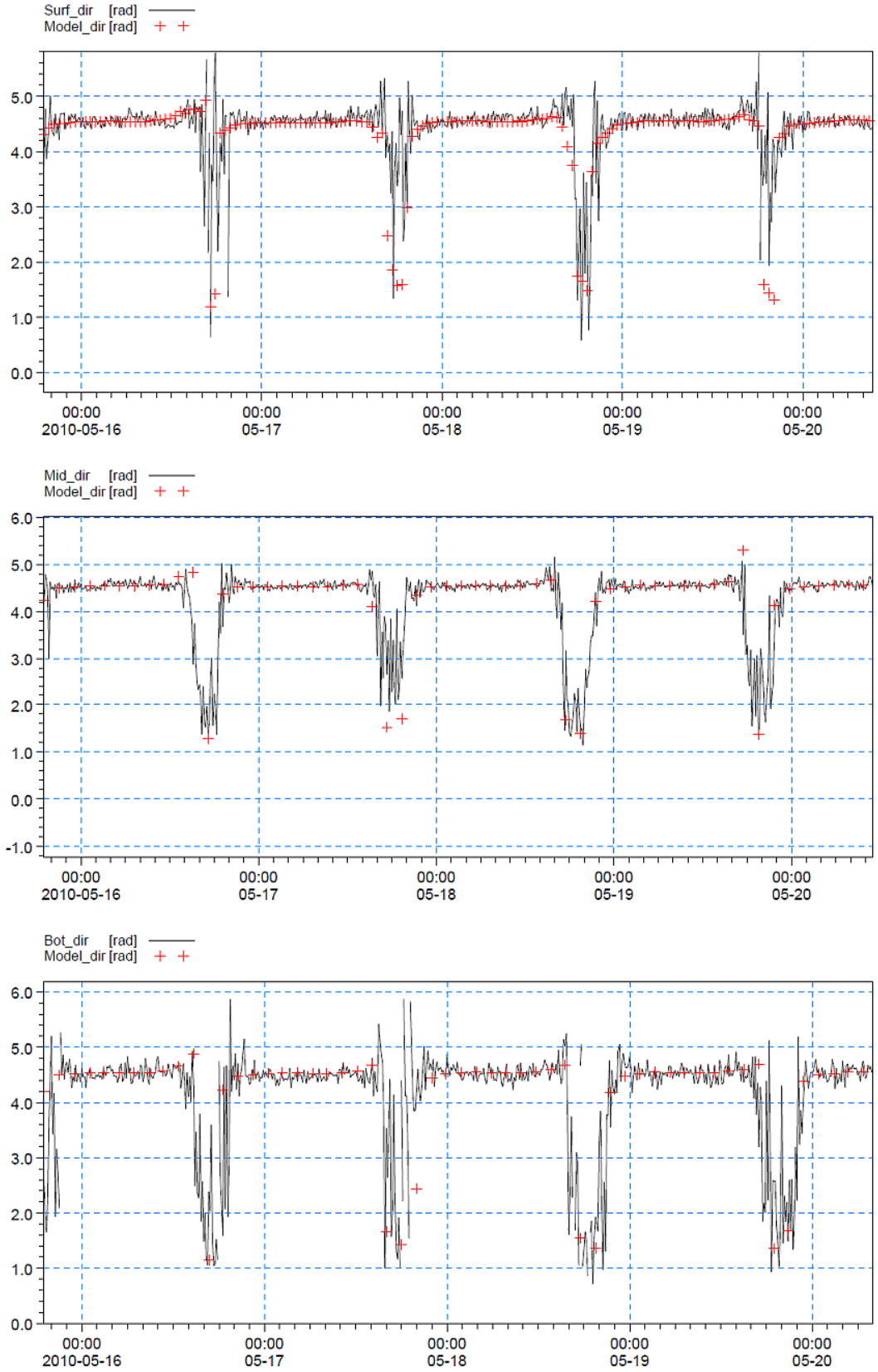

Figure 70. Calibration results showing good agreement between the observed current directions (line) of the surface layer (top panel), mid water layer (central panel), and near-bed layer (bottom panel), and those obtained from the model (crosses) for the ADP location in the channel.

4 References

Department of Commerce. 2009. Affirmation of Vertical Datum for Surveying and Mapping Activities for the Islands of Rota, Saipan and Tinian of CNMI. *Notice published in Federal Register* 74 (13), p.3990.

Dickinson, W.R. 2000. Hydro-Isostatic and tectonic influences on emergent Holocene paleoshorelines in the Mariana Islands, Western Pacific. *Journal of Coastal Research* 16(3), 735-746.

ECMWF. 2007. IFS Documentation – Cy31r1, Part VII: ECMWF Wave Model. ECMWF, 56p.

Smithers, S.G. and Woodroffe, C.D. 2000. Microatolls as sea-level indicators on a mid-ocean atoll. *Marine Geology* 168, 61-78.